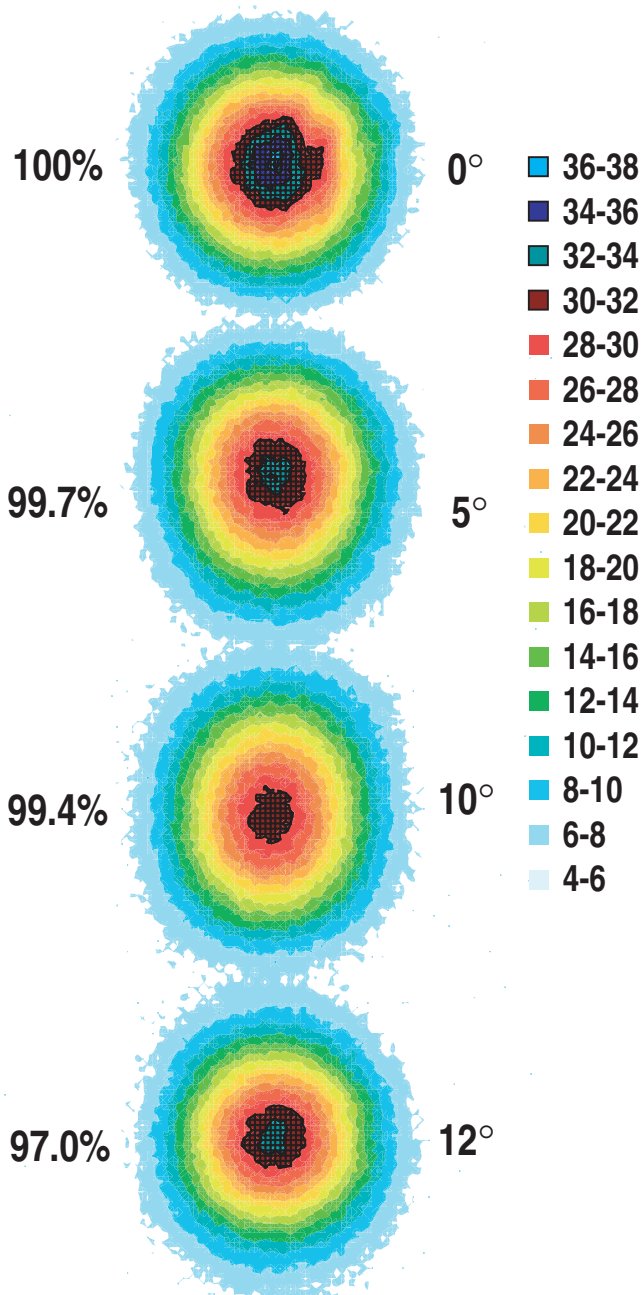


FUSION RESEARCH AT GENERAL ATOMICS

ANNUAL REPORT

*ADVANCED FUSION
TECHNOLOGY RESEARCH
AND DEVELOPMENT*



*OCTOBER 1, 2001
THROUGH
SEPTEMBER 30, 2002*

DISCLAIMER

This report was prepared as an account of work sponsored by an agency of the United States Government. Neither the United States Government nor any agency thereof, nor any of their employees, makes any warranty, express or implied, or assumes any legal liability or responsibility for the accuracy, completeness, or usefulness of any information, apparatus, product, or process disclosed, or represents that its use would not infringe privately owned rights. Reference herein to any specific commercial product, process, or service by trade name, trademark, manufacturer, or otherwise, does not necessarily constitute or imply its endorsement, recommendation, or favoring by the United States Government or any agency thereof. The views and opinions of authors expressed herein do not necessarily state or reflect those of the United States Government or any agency thereof.

This report has been reproduced
directly from the best available copy

Available to DOE and DOE contractors from the
Office of Scientific and Technical Information

P.O. Box 62

Oak Ridge, TN 37831

Prices available from (615) 576-8401,

FTS 626-8401

Available to the public from the
National Technical Information Service

U.S. Department of Commerce

5285 Port Royal Road

Springfield, VA 22161

Cover Photo: Results of low power measurements made at JAERI on remotely steerable lancer apparatus. See Section 9.2.

GA-A24304

**ADVANCED FUSION TECHNOLOGY
RESEARCH AND DEVELOPMENT**

**ANNUAL REPORT TO THE
U.S. DEPARTMENT OF ENERGY**

OCTOBER 1, 2001 THROUGH SEPTEMBER 30, 2002

**by
PROJECT STAFF**

**Work prepared under
Department of Energy
Contract No. DE-AC03-98ER54411**

**GENERAL ATOMICS PROJECT 30007
DATE PUBLISHED: DECEMBER 2003**



TABLE OF CONTENTS

1. ADVANCED FUSION TECHNOLOGY RESEARCH AND DEVELOPMENT OVERVIEW	1-1
2. FUSION POWER PLANT STUDIES (ARIES)	2-1
2.1. Background	2-1
2.2. Target Fabrication	2-1
2.3. Target Chamber Aerosol Limits	2-2
2.4. Target Mechanical Properties Estimate	2-2
2.5. Conferences and Meetings	2-3
3. IFE CHAMBER ANALYSIS	3-1
3.1. Conferences/Meetings	3-2
3.2. Publications	3-2
4. IFE TARGET SUPPLY SYSTEM	4-1
4.1. Background	4-1
4.2. FY02 Scope and Objectives	4-1
4.3. Major Facility Upgrade	4-1
4.4. Target Fabrication	4-2
4.5. Target Injection	4-3
4.6. GA Hosted Meetings	
4.6.1. US/Japan Target Fabrication and Injection Workshop	4-4
4.6.2. GA/LANL Presentations at the US/Japan Workshop	4-5
4.6.3. IAEA Targets and Chambers Meeting	4-5
4.6.4. GA/LANL Presentations at the IAEA Meeting	4-5
4.7. Conferences/Meetings	4-6
4.8. Publications/Reports	4-6
5. NEXT STEP FUSION DESIGN	5-1
5.1. Physics	5-1
5.1.1. E3 Physics Operations	5-1
5.1.2. Experimental Program Topics, Sequence and Pulse Number	5-2
5.1.3. In-Vessel Tritium Retention Issues	5-6
5.2. Engineering	5-9

5.3.	Thermal Analysis of FIRE Divertor	5-11
5.3.1.	Thermal Stress Analysis	5-11
5.3.2.	Thermal Hydraulic Analysis Results	5-12
5.3.3.	Thermal Fatigue Analysis of FIRE Divertor Segment	5-13
6.	ADVANCED LIQUID PLASMA SURFACE	6-1
6.1.	Modeling	6-1
6.2.	Li MHD Modeling and Analysis	6-2
6.3.	Li-DiMES Experiment	6-2
6.4.	Atomic Data	6-2
6.5.	Conferences/Meetings	6-3
7.	ADVANCED POWER EXTRACTION STUDY	7-1
7.1.	SiC _f /SiC Design Assessment	7-1
7.2.	Ferritic Steel Design	7-1
7.3.	AFS/Flibe First Wall and Blanket Design	7-1
7.4.	Thermal Hydraulics Assessment	7-2
7.5.	Conferences/Meetings	7-5
7.6.	Publications	7-6
8.	PLASMA-FACING COMPONENTS — DiMES	8-1
8.1.	DiMES Mechanism	8-1
8.2.	DIII-D Experiments	8-1
8.3.	Experiment in C-Mod	8-2
8.4.	Chamber Recycling	8-2
8.5.	Analysis of Ne Injection Detachment	8-2
8.6.	Smart Tile Concept	8-5
8.7.	Conferences/Meetings	8-5
8.8.	Publications	8-5
9.	RF TECHNOLOGY	9-1
9.1.	Compline Antenna	9-1
9.2.	Advanced ECH Launcher Development	9-2
9.3.	International Collaboration	9-4
9.4.	Conferences/Meetings	9-4
9.5.	Publications	9-4

LIST OF FIGURES

2-1.	Scattering and extinction efficiencies versus sphere radius	2-3
2-2.	Aerosol mass densities for Pb or Fluorine salts	2-3
4-1.	The IFE target fabrication and injection facility	4-2
4-2.	Concept for target fabrication	4-3
4-3.	Participants in the US/Japan IFE Target Fabrication and Injection Workshop	4-4
5-1.	ITER plan and cumulative FW fluence	5-7
5-2.	Features of FIRE baseline	5-10
7-1.	APEX recirculating blanket tokamak reactor, poloidal module and FW blanket cross-section	7-3
7-2.	FW/blanket cross-section and coolant routing	7-3
8-1.	Measured net carbon erosion along a line in the radial direction	8-3
9-1.	Comblane antenna for use on LHD at NIFS	9-1
9-2.	Results of low power measurements made at JAERI on remotely steerable launcher apparatus	9-3

LIST OF TABLES

5-1.	Device-specific data	5-3
5-2.	FIRE 16-year plan summary	5-5
5-3.	Ignitor 10-year operation plan summary	5-6
5-4.	ITER operation plan summary	5-6
5-5.	Estimated in-vessel T retention and FPEs to reach in-vessel limit	5-8
5-6.	Features of the ITER central solenoid	5-11
5-7.	Results of thermal hydraulic analysis	5-13
5-8.	Flux distribution time curve	5-14
5-9.	Temperature dependent material properties for unirradiated Cu-Cr-Zr	5-14
7-1.	Thermal hydraulics parameters of the inboard and outboard FW/blanket modules	7-4

1. ADVANCED FUSION TECHNOLOGY RESEARCH AND DEVELOPMENT OVERVIEW

The General Atomics (GA) Advanced Fusion Technology program seeks to advance the knowledge base needed for next-generation fusion experiments and, ultimately, for an economical and environmentally attractive fusion energy source. To achieve this objective, we carry out fusion systems design studies to evaluate the technologies needed for next-step experiments and power plants, and we conduct research to develop basic and applied knowledge about these technologies. GA's Advanced Fusion Technology program derives from, and draws on, the physics and engineering expertise built up by many years of experience in designing, building, and operating plasma physics experiments. Our technology development activities take full advantage of the GA DIII-D program, the DIII-D facility and the Inertial Confinement Fusion (ICF) program and the ICF Target Fabrication facility.

The following sections summarize GA's FY02 work in the areas of Fusion Power Plant Studies (ARIES, Section 2), Inertial Fusion Energy (IFE) Chamber Analysis (Section 3), IFE Target Supply System Development (Section 4), Next Step Fusion Design (Section 5), Advanced Liquid Plasma Facing Surfaces (ALPS, Section 6), Advanced Power Extraction Study (APEX, Section 7), Plasma Interactive Materials (DiMES, Section 8) and RF Technology (Section 9). Our work in these areas continues to address many of the issues that must be resolved for the successful construction and operation of next-generation experiments and, ultimately, the development of safe, reliable, economic fusion power plants.

Our work was supported by the Office of Fusion Energy Sciences, Facilities and Enabling Technologies Division, of the U.S. Department of Energy.

2. FUSION POWER PLANT STUDIES (ARIES)

2.1. BACKGROUND

The ARIES Program is a multi-institutional activity to explore and develop the commercial potential of fusion as a future energy source. This is accomplished through integrated systems studies of both MFE and IFE power plant concepts. General Atomics' task is to provide target injection and target fabrication input to the ARIES-IFE integrated system studies.

We participated in the ARIES IFE meetings listed in the following sections as well as monthly conference calls. We hosted the summer ARIES meeting for 21 participants at General Atomics on July 1–2, 2002. The ARIES study emphasized the dry wall chamber through the early part of this reporting period and moved on to the wetted wall design later in the year. We provided updates on target fabrication and injection research and participated in target and chamber design guidelines as they affect target fabrication and injection. In this regard, we often brought results to ARIES meetings and reported ongoing work regardless of funding source.

2.2. TARGET FABRICATION

We proposed an ARIES task to systematically evaluate the issues associated with the selection of hohlraum materials for the Heavy Ion Fusion (HIF) target and optimize the materials from the view of a viable power plant system. The selection of hohlraum materials for the HIF target is a significant feasibility issue as it must satisfy many multi-disciplinary requirements. This topic is still an “open question” in the HIF community. The materials selected affect many critical aspects of an IFE power plant system. They have a direct effect on:

- Target physics for target gain.
- Cost and complexity (even feasibility) of target fabrication.
- Cost of equipment and operations to remove the materials from the Flibe.
- Compatibility of structural materials with hohlraum components (e.g., primary loop corrosion).
- Radioactive inventory of materials.
- Handling operations in the plant (glove box or remote handling, remote maintenance of equipment).

- Decisions to recycle materials or discard them (waste volume, high-level waste generation).
- Heat transfer for layering the targets (if in-hohlraum layering is used).
- Acceleration limit for injecting the targets (strength of materials in needed density and geometry).

We presented the methodology leading to an estimated cost of 16.6 cents/target for NRL direct drive targets.

2.3. TARGET CHAMBER AEROSOL LIMITS

We estimated the effects of aerosols in the chamber on target injection and tracking. For heavy ion driven targets the particle size limit is about 0.2 mg, or ~0.3 mm radius to avoid changing the target's axial trajectory by more than 0.3 mm and thereby avoid the need for in-chamber tracking. The corresponding density limit for many smaller droplets is about 1 g/m³. Aerosols in direct drive chambers will have to be much smaller if they would stick to the target surface. A conservative requirement would suggest that particle size be limited to about 50 nm to maintain a 50 nm surface finish. Larger particles may be acceptable if they flatten substantially on impact. Also, high Z surface build up should be limited to about 3 nm, which would limit Pb aerosol density to about 5 mg/m³.

We calculated the effects of aerosols on tracking and laser driver beam absorption, scattering and extinction. The limiting particle density versus particle size for Pb and Flibe aerosols were calculated. We estimated the light scattering and extinction of Flibe aerosols in an IFE chamber using the index of refraction of other representative fluorine salts (n=1.4, k=0). As shown in Fig. 2-1, for a particle size much less than the light wavelength, the light extinction for fluorine salt was found to be much less than for Pb aerosols. Therefore, the number density limits for small Flibe aerosols that would absorb a given fraction of a light beam are much higher than those for Pb aerosols. As shown in Fig. 2-2, the mass density limit is about 10⁻⁸ g/cm³ (10 mg/m³ dependent on particle radius) based on tracking and driver beam extinction (10% absorption or scattering while passing to the center of a 6.5 m radius chamber).

2.4. TARGET MECHANICAL PROPERTIES ESTIMATE

Simple estimates for mechanical properties of foams that could be used for target insulation were made and compared to estimated DT mechanical properties. These calculations indicated that rather low-density foams could be used without degrading outer target strength for handling and acceleration. Roughly 7% dense plastic foams would have Young's modulus equal to that of DT and 1% dense foam would have collapse stress equal to the estimated yield stress of DT at target temperatures.

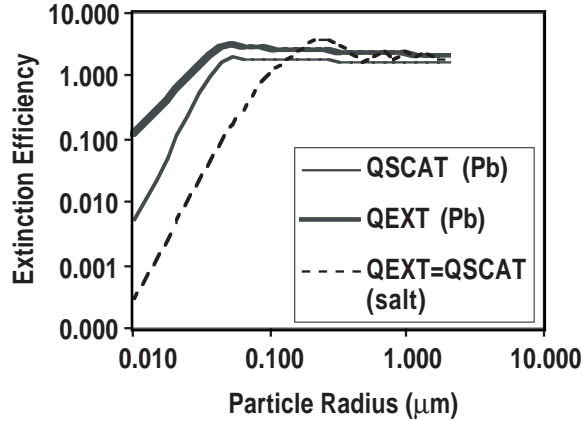


Fig. 2-1. Scattering and extinction efficiencies versus sphere radius.

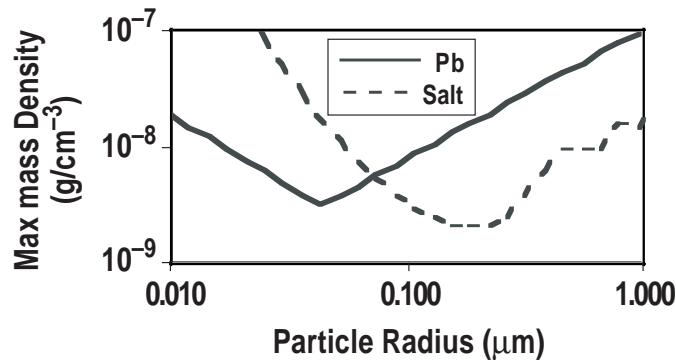


Fig. 2-2. Aerosol mass densities for Pb or Fluorine salts that would absorb or scatter 10% of a light beam passing to the center of a 6.5 m radius chamber.

2.5. CONFERENCES AND MEETINGS

ARIES project meeting on January 10–11, 2002, San Diego, California. Presented “Target Injection in Sacrificial Wall/Aerosol-Filled Chambers” and “Progress in IFE Target Fabrication”.

ARIES project meeting on April 22–23, 2002, Madison, Wisconsin. Presented “Aerosol Limits for Target Tracking”.

ARIES project meeting on July 1–2, 2002, GA, San Diego, California. Presented “Update on Target Fabrication, Injection, and Tracking”.

ARIES project meeting on October 2–4, 2002, Princeton, NJ. Presented “Indirect-drive Target Aerosol Limits, Foam Mechanical Properties, and Target Injection Accuracy”.

3. IFE CHAMBER ANALYSIS

This task assists the national fusion program in the identification, analysis, and evaluation of critical issues for the chamber technology for both MFE and IFE; enhances the synergism in research and development planning and execution for the chamber technology issues that are common to both IFE and MFE; and helps initiate technical collaboration among scientists in the U.S. and other countries on innovative chamber technology concepts.

The chamber technology components for MFE and IFE have some unique as well as common issues. In addition, the U.S. Fusion Energy Sciences Program has encouraged initiatives to enhance science and innovation. For example, liquid walls have long been proposed in IFE. More recently, liquid walls are being explored under MFE-oriented APEX and ALPS projects.

Liquid walls offer excellent opportunities to enhance the attractiveness of fusion energy systems by handling high power density, reducing activation, increasing device availability, and simplifying material and technological constraints. However, liquid walls have many scientific and engineering issues that require experiments, modeling, analysis, and design. Since the resources available to both IFE and MFE in the chamber technology area are very limited, both programs benefit from clearly identifying the common issues and enhancing synergism in the R&D.

Continuing progress has been made in exploring and identifying innovative concepts for the chamber technology. Assessments of variations for flowing liquid walls was conducted. Concepts to extend the power density and operating temperature capability were evaluated. Scientific and engineering issues were identified, and efforts to resolve these issues continue. Collaboration with Japan and Europe has evolved and important technical information exchanges were successful.

Technical issues investigated/assessed:

- Flinabe properties, including heat transfer and surface waves.
- Flibe vaporization.
- Flinabe (LiF-NaF-BeF₂) versus Flibe (LiF -BeF₂).
- Molten salt heat transfer.
- Low-K heat transfer.
- Vapor dynamics and vapor condensation.
- IFE chamber clearing.

- Stability of liquid jets.
- Beam swirl flow.
- Fluid dynamics scaling.
- Thermofluid issues and facility evaluation.
- Interfacial transport.
- Free surface flow.
- MHD Turbulence.
- Liquid wall penetrations, nozzles, R&D requirements.
- Safety issues.

FY02 accomplishments:

- Modeling needs for low conductivity fluids were assessed.
- MHD models for liquid metals were evaluated.
- Facility needs for chamber issues were evaluated.

3.1. CONFERENCES/MEETINGS

1. ALPS/APEX Project Meeting, Scottsdale, Arizona, November, 2001.
2. US-Japan International Workshop on Innovative Concepts, Osaka, Japan, May 2002.

3.2. PUBLICATIONS

M.A. Abdou and The APEX TEAM, "On the Exploration of Innovative Concepts for Fusion Chamber Technology," *Fusion Engineering and Design* **54:2**, 181 (2001).

4. IFE TARGET SUPPLY SYSTEM

4.1. BACKGROUND

The overall purpose of this task is to address issues associated with the target supply system for a future IFE power plant. This includes the major areas of target fabrication,¹ injection, and tracking. The long-term workscope for this task is to address the following issues:

- Ability to economically fabricate, fill, and layer targets that meet IFE requirements.
- Ability of targets to withstand acceleration into the reaction chamber.
- Ability of targets to survive in the chamber environment (heating due to radiation and gases).
- Accuracy and repeatability of target injection.
- Ability to accurately track targets.

4.2. FY02 SCOPE AND OBJECTIVES

This work is for indirect-drive targets, or tasks that are generic to either indirect or direct drive targets. Work on laser driven direct-drive target fabrication and injection is being accomplished under separate funding from the Naval Research Laboratory.

Major accomplishments under this scope of work:

- The fast acting propellant gas valve design and construction was completed.
- We hosted the U.S./Japan target fabrication and injection workshop.
- We hosted the IAEA Technical Meeting on the Physics and Technology of Inertial Fusion Energy Targets and Chambers.
- We participated in the Snowmass 2002 Fusion Energy Sciences Summer Study.

4.3. MAJOR FACILITY UPGRADE

While not conducted with OFES funding, a major milestone was completed this year – renovation of the former TRIGA fuel fabrication building for Inertial Fusion target

¹GA is supporting LANL, which is the lead lab for target fabrication.

fabrication and injection research. Modular office space and a parking lot was also provided next to this building. Figure 4–1 includes photographs from April and December 2002 that indicate the extensive upgrades that were completed.



Fig. 4–1. The IFE target fabrication and injection facility before and after renovation.

4.4. TARGET FABRICATION

A combination of Hf, Hg, Xe, and Kr has been suggested for the outer hohlraum wall of a heavy ion fusion target, as materials that would give good target physics performance and be separable from Flibe in an IFE power plant. These elements include a solid, liquid, and two noble gases and may be more costly to fabricate.² However, they are all solids at cryogenic temperatures and it might be possible to apply layers of these materials at successively lower temperatures. If they are applied in layers, the layers will probably have to be less than a few hundred nanometers thick, to achieve the desired physics properties. They might also be pressed together from powders or molded.

Working with target designers we have identified, for the first time, potential manufacturing processes from beginning to end for the distributed radiator HIF target. We

²For example, cryogenic handling from the first step of the manufacturing process would be required.

conducted a survey of high-Z, low-density foam manufacturing methods for the absorber/radiators in the HIF target. We performed a chemical engineering analysis of an “nth-of-a-kind” target fabrication facility for the HIF target. We completed cost estimates (\$0.11 per target) for fabrication of a polystyrene ablator, filled and layered with DT. We estimated the cost of producing all hohlraum components by laser chemical vapor deposition (LCVD). A hohlraum such as illustrated in Fig. 4–2 could be fabricated from the inside to the outside using LCVD with an injection molded outer case. The total baseline estimate is \$0.41 per injected target for a 1000 MW (electrical) plant.

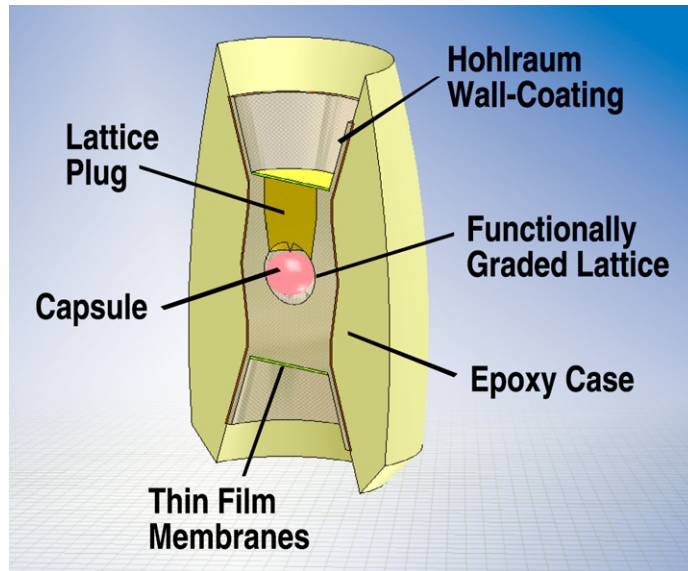


Fig. 4–2. Concept for target fabrication from the inside out using LCVD with a molded epoxy case (LANL).

4.5. TARGET INJECTION

Oak Ridge National Laboratory completed design, fabrication, and testing of the propellant gas valve under contract to GA with OFES funding. This valve provides high speed (2 ms open or shut) with high flow rate (for up to 400 m/s target speed) and low pressure-drop operation.

With Naval Research Laboratory funding, we completed fabrication of most of the components required for single shot target injection with single axis tracking. Most of these components can be used for both direct-drive and indirect-drive targets.

We researched methods for estimating mechanical properties of low-density materials (Pb/Hf radiators in the hohlraum) in indirect drive targets. We started development of a computer model to calculate stress in an indirect drive IFE target under acceleration.

4.6. GA HOSTED MEETINGS

4.6.1. US/Japan Target Fabrication and Injection Workshop

We hosted the US/Japan IFE Target Fabrication and Injection Workshop December 3–4, 2001. About 20 specialists from the U.S. and Japan participated (workshop photograph in Fig. 4–3), presenting recent work and program overviews. A CD was prepared and distributed with the presentations from the meeting. We agreed to a more extensive cooperation program over the next few years — including working visits for personnel, exchange of targets for characterization, and additional working meetings. The following specific action items were agreed upon.

1. Continued workshops on an annual basis:
 - December 2002 in San Diego, ~1 week workshop in U.S. to include small-group brainstorming sessions to focus on specific problems of each participant (took place in February 2003).
2. Personnel exchanges
 - Year 1 — U.S. person visit ILE target fabrication labs (several week working assignment; took place in April 2003).
 - Year 2 — Japan person to work with target injector at GA.
3. Japan to send samples to U.S. for characterization (e.g., transparent shells).
4. U.S. provide characterization of samples (e.g., spheremapper, wallmapper).
5. Collaborate on a “Moore’s Law for Targets” publication (in progress).



Fig. 4–3. Participants in the US/Japan IFE Target Fabrication and Injection Workshop.

4.6.2. GA/LANL Presentations at the US/Japan Workshop

- D.T. Goodin, “IFE Target Fabrication and Injection at GA”.
- R.W. Petzoldt, “Target Injection for IFE”.
- N.B. Alexander. “Target Supply Systems for Z-pinch IFE”.
- S. Willms, “Overview of IFE activities at LANL”.
- B. Rickman, “Chemical Process Modeling for Target Fab Scaleup”.
- J. Hoffer, “Cryo Layering for IFE Applications”.
- A. Greenwood and E. Stephens, “High-Z coatings for Targets”.
- W. Steckle, “Polymer Foam Developments for IFE target Fabrication at LANL”.
- N. Alexander, “Advanced Target Concepts for Survival During Injection”.
- L. Brown, “Fluidized Beds for IFE Target Fabrication”.
- C. Halvorson, “Cryogenic Fuel Layering for IFE”.

4.6.3. IAEA Targets and Chambers Meeting

We hosted the IAEA Technical Meeting on Physics and Technology of Inertial Fusion Energy Targets and Chambers. The meeting took place at General Atomics on June 17–19, 2002. Sixty-eight U.S. and international visitors from the inertial fusion community attended. We collected presentations from the meeting participants and posted them to the web site <http://web.gat.com/conferences/iaea-tm/main.html> for access by all. As guest editor for a special issue of Fusion Science and Technology, we collected 33 papers, selected reviewers for each paper, collected the reviews and returned them to the authors with our change recommendations. Four of these papers were prepared at General Atomics.

4.6.4. GA/LANL Presentations at the IAEA Meeting

- J. Dahlburg, “Target Fabrication — Its Role in High Energy Density Plasma Phenomena”.
- J. Hoffer, “Studies of DT in IFE Targets”.
- W. Rickman, “Filling and Layering Research of Inertial Fusion Targets in the LANL Cryogenic Pressure Loader”.
- E. Valmianski, “Wake Shields for Protection of IFE Targets During Injection”.
- R. Petzoldt, “Experimental Target Injection and Tracking System”.
- E. Stephens, “Palladium and Palladium Gold Alloys as High Z Coating for IFE Targets”.

- N. Alexander, “Layering of IFE Targets Using a Fluidized Bed”.
- W. Steckle, “Low Density Materials for use In Inertial Fusion Targets”.
- A. Greenwood, “Thickness and Uniformity Measurements of Thin Sputtered Gold Layers on ICF Capsules”.

4.7. CONFERENCES/MEETINGS (NOT AT GA)

- **14th International Symposium on Heavy Ion Inertial Fusion**

In Moscow, Russia, May 26–31, 2002. We prepared and presented the paper “A Credible Pathway for Heavy Ion Driven Target Fabrication and Injection”.

- **Snowmass 2002 Fusion Energy Sciences Summer Study**

In Snowmass, Colorado, July 18–29, 2003. We prepared and presented “Membrane Support of Targets” and “Status of Target Fabrication and Injection”.

4.8. PUBLICATIONS/REPORTS

Goodin, D.T., C.R. Gibson, R.W. Petzoldt, N.P. Siegel, L. Thompson, A. Nobile, G.E. Besenbruch, K.R. Schultz, “Developing the Basis for Target Injection and Tracking in Inertial Fusion Energy Power Plants,” *Fusion Engineering and Design* **60**, 27 (2002).

Goodin, D.T., A. Nobile, N.B. Alexander, R.W. Petzoldt, “Progress Towards Demonstrating IFE Target Fabrication and Injection,” presented at the 2nd Int. Conf. on Inertial Fusion Science and Applications 2001, to be published in *Fusion Technology*; General Atomics Report GA–A23832 (2003).

Petzoldt, R.W., N.B. Alexander, T.J. Drake, D.T. Goodin, K. Jonestrask, R.W. Stemke, “Experimental Target Injection and Tracking System,” to be published in *Fusion Technology* (2003).

Goodin, D.T., A. Nobile, N.B. Alexander, L.C. Brown, J.L. Maxwell, J. Pulsifer, A.M. Schwendt, M. Tillack, and S.W. Willms, “A Credible Pathway for Heavy Ion Driven Target Fabrication and Injection,” *Laser and Particle Beams* **20**, 515 (2002).

Goodin, D.T., A. Nobile, J. Hoffer, A. Nikroo, G.E. Besenbruch, L.C. Brown, J.L. Maxwell, W.R. Meier, T. Norimatsu, J. Pulsifer, W.S. Rickman, W. Steckle, E.H. Stephens, M. Tillack, “Addressing the Issues of Target Fabrication and Injection for Inertial Fusion Energy,” *Proc. 22nd Symp. on Fusion Technology*, Helsinki, Finland, 2002, to be published in *Fusion Engineering and Design*.

- A.M. Schwendt, A. Nobile, P. Gobby, W.P. Steckle, D., Colombant, J.D. Sethian, D.T. Goodin, G.E. Besenbruch, "Tritium Inventory of Inertial Fusion Energy Target Fabrication Facilities; Effects of Foam Density and Consideration of Target Yield of Direct Drive Targets," *Fusion Science and Technology* **43**, 217 (2002).
- W.R. Meier, B.G. Logan, W.L. Waldron, G.L. Sabbi, D.A. Callahan, P.F. Peterson, D.T. Goodin, "Progress Toward Heavy-Ion IFE," *Fusion Engineering and Design* **63–64**, 577 (2002).

5. NEXT STEP FUSION DESIGN

This task provides physics analysis and other scientific and technical input to Next Step Options (NSOs) Studies for the U.S. Fusion Science Program. Emphasis in this work is on options (design candidates) to obtain plasma behavior at high energy gain and for long duration operation pulses. The principal content of the Task is to provide definition of physics and plasma operation objectives, physics and plasma science assessments and definition of physics and other design requirements for U.S. NSO studies.

5.1. PHYSICS

Activity for this task comprises an approximately 0.1 FTE effort and has been conducted on an approximately constant level-of-effort basis. John Wesley is the principal and sole investigator at GA.

NSO physics activities during FY02 included participation in the Preliminary Organizing Committee meetings for the 2002 Fusion Science Summer Study (Snowmass 2002) held at Snowmass Village, Colorado, in July 2002. Wesley co-chaired the Magnetic Fusion Energy (MFE) “Physics Operations” Working Group and also worked with GA Fusion Group computer support personnel to set up the Snowmass 2002 website <http://web.gat.com/snowmass/> on the GA Fusion web server.

A comprehensive report of the data compiled by the E3 “Physics Operations” Working Group was prepared and forwarded to the Summer Study Final Report Secretaries [John DeLooper and Ned Sauthoff at Princeton Plasma Physics Laboratory (PPPL)]. Selected highlights from this final report are shown below.

5.1.1. E3 Physics Operations

The E3 Physics Operations Working Group (WG) comprised one of four experimental program-related WGs convened under the aegis of the MFE Experimental Approach and Objectives Working Group during the 2002 Fusion Energy Sciences Summer Study held at Snowmass Village, Colorado, 8–19 July 2002.

Membership of the E3 WG comprised Peter Petersen (GA), Al Hyatt (GA), Dave Humphreys (GA), Eric Fredrickson (PPPL), Mike Bell (PPPL), Dennis Mueller (PPPL), Charles Skinner (PPPL) and Jo Lister (CRPP-EPFL). Device spokespersons who provided data and input for the WG’s deliberations before and during the Summer Study included Dale Meade (PPPL), for FIRE; B. Coppi (MIT), F. Bombarda (MIT), and L. Sugiyama (MIT), for

Ignitor; and Rip Perkins (PPPL) and R. Parker (MIT) for ITER. Representatives of the ITER international team, G. Federici in particular, also made significant contributions to the WG's deliberations during the Summer Study.

John Wesley was responsible for E3 WG organization and data compilation before the Summer Study. Dave Humphreys and Arnie Kellman (GA) chaired the E3 plenary and breakout sessions during the Summer Study and prepared the Summary Report. John Wesley compiled, edited and formatted the Final Report.

The charter and scope for the E3 WG was to examine generic Burning Plasma Experiment (BPX) matters that apply to the hourly, daily, annual and lifetime operation of device and facility to conduct plasma science studies and experimentation in the “burning plasma regime”, where Q is ≥ 10 . $Q = 10$ is nominal; the range of scientific interest is $Q = 5$ to infinity.

The content of the resulting Final Report was organized by topic into four subsequent sections:

- Section 2. Experimental Program Topics, Sequence and Pulse Number
- Section 3. In-Vessel Tritium Retention Issues
- Section 4. Divertor and/or Limiter PFC Lifetime Issues
- Section 5. Plasma Shape Control and Flexibility Issues

There were also six individually authored supporting appendices:

- A1.1. Halo Current Disruption Loads in ITER, FIRE, and Ignitor
- A1.2. Prospects for Mitigation of Disruption Heat Loads and Runaway Electrons Using High-Pressure Gas Injection
- A1.3. Disruption Causes and Frequency
- A2.2. Present Non-BP Experimental Operation Attributes
- A3.1. Tritium Parameters and Usage/Inventory Issues
- A3.2 Tritium-Related Constraints on BPX Operation

A summary of the data and key issue discussion regarding Sections 2 and 3 follow.

5.1.2. Experimental Program Topics, Sequence and Pulse Number

All BPXs will progress through a “classical” sequence of device and commissioning and operation that will culminate with use of the device and facility for the conduct of “user-driven” burning plasma science experiments and technology development studies. This “user/science-study/technology-test phase” will follow after an extended initial period of device systems commissioning and burning plasma operation development. This

development of routinely attainable burning plasma operation will, in itself, constitute an integrated test of the respective device's science and technology bases. These bases are not identical among the three candidate devices, so which physics and technology aspects will be tested in this integration phase will vary.

Table 5–1 summarizes device-specific data relevant to a general overview understanding of the three BPXs and to E3 consideration of their respective operational aspects.

Table 5–1
Device-Specific Data

Attribute (Units)	FIRE	Ignitor	ITER
R_0 (m)	2.14	1.32	6.20
a (m)	0.595	0.47	2.00
A (R_0/a)	3.60	2.81	3.10
ϵ (a/R_0)	0.278	0.386	0.323
Plasma configuration	DN divertor	Inner wall limiter	SN divertor
κ_{95}	~1.8	—	1.70
κ_x or κ_a	~2.0	1.83	1.85
δ_{95}	~0.4	—	0.33
δ_x or δ_a	~0.7	0.4	0.49
B_T (T)	10	13	5.3
I_p (MA)	7.7	11	15 (17)
q_{95}	3.0	—	3.0 (~2.6)
q_a	—	3.6	—
TF type	80K BeCu/Cu	30K Cu	5K NbSn CICC
TF flattop (s)	21	~4	steady-state
TF rep rate (hr^{-1})	0.33	~0.33 ?	steady-state
TF pulses (full field)	≥ 3000	3000 ???	NA
PF type	80K OFHC Cu	30K Cu	5K NbSn CICC
PF rep rate (hr^{-1})	0.33	0.33 ???	1.6
Fusion power (MW)	150	100	500
Fusion burn duration (s)	~20	~4	~440
Limiting system(s)	TF, PF, PF(V-s)	TF, PF, PF(V-s)	PF(V-s)
FPE energy (GJ) (Full Power Equiv.)	3.0	0.4	220
VV/FW area (m^2)	~80	~36	~720
Γ_n (MW/m^2)	1.5	2.2	0.57
P_{aux} (MW)	20	20	73
P_{aux} Type	ICRF	ICRF	NNBI + ICRF + ECRF

Table 5–1 (Cont.)

Attribute (Units)	FIRE	Ignitor	ITER
τ_E (s) (including radiation loss)	~1.0	~0.62	3.4
W_{th} (MJ)	~35	12	353
$\langle\beta\rangle$ (%)		1.2	2.8
β_N	~1.8 (?)	~1	2.0
T burnup per FPE pulse (g)	0.005	0.0007	0.40
FPE per year	216	150–300	2,000–3,000
Annual T burnup (g)	1.2	0.11	800
T fueling input (g) per FPE pulse	0.7–1.0	0.08	240
Annual once-through T fueling input (g)	220	12-24	470,000
On-site T inventory limit (g)	30	10 (?)	3,000
On-site T reprocessing	Yes; ≥ 0.1 g/hr	Yes (?)	Yes; 480 g/hr
FW cumulative energy (GJ/m ²)	34	6.3	2,900
FW neutron fluence (MW/a ²), at end of initial operation period	0.0011	0.0002	0.094
FW fluence limit (MW/a ²) (design basis)	~0.003	?	0.3

5.1.2.1. Fusion Ignition Research Experiment (FIRE). FIRE (<http://fire.pppl.gov>) is a high-field (10-T) compact BPX based upon 80K adiabatically cryocooled copper TF and PF magnets, with actively cooled in-vessel divertor PFCs. Nominal plasma current is 7.7 MA. Nominal operation is targeted towards 20-s Q = 10 DT burn, with fusion power of 150 MW, initiated and sustained with up to 20 MW of ICRF heating. The inertial heat capacities of the TF and PF magnets allow the possibility of longer-pulse, reduced-B and/or reduced- I_p operation in “standard” and “advanced tokamak” modes. As summarized in Table 5–2, comprehensive physics and in-vessel component technology study program is planned.

5.1.2.2. Ignitor. Ignitor (<http://www.frascati.enea.it/ignitor/>) is a very-high-field (13 T), maximally compact BPX based upon 30K adiabatically cryocooled copper TF and PF magnets, with adiabatically cooled in-vessel limiter PFCs. Nominal plasma current is 11 MA. Nominal operation is targeted towards fully ignited DT burn with fusion power of 100 MW, facilitated and sustained (if necessary) with ICRF heating of up to 24 MW. The inertial heat capacity of the TF and PF magnets will allow the possibility of longer-pulse, reduced B

and/or I_p operation in “standard” and “advanced tokamak” modes. An ignition physics study program is planned.

Table 5–2
FIRE 16-Year Plan Summary

Phase	Years After First Plasma	Activities/Benefits
Commissioning (H,D)	0–3	Control, cleanup, fueling, diagnostics, operations, ICRF tests; RH checkout
DT H–mode Transient AT and ITB	4–6	Initial ICRF heating, plasma power handling, initial physics studies; alpha heating, energy transport, fast particle, particle and ash exhaust; global burn control, transient profile control, transient AT
Upgrade	7	Install LHCD
DT Optimized H–mode; AT control and optimization	8–16	Optimization of AT modes, non-inductive profile control, improve divertor and FW power handling, extend pulse length
Program completion	16	T burn-up $\cong 13$ g $\Gamma_n = 0.003$ Mwa/m ²

The plan, summarized in Table 5–3, comprises ~23,000 total machine pulses, with ~7000 H “commissioning and development” pulses in the first two years, ~10,600 DD development and pre-DT setup pulses, principally in the final 8 years, and ~3000 95%-D+5%-T and 1770 50%-50% DT performance pulses, principally in the final 6 years. In all cases, operation commencing in Year 5 encompasses an interleaved mixture of DD and 95D-5T setup pulses and 50-50 DT performance pulses. The cumulative 14 MeV yield becomes appreciable by Year 5 and reaches $\sim 10^{23} = 2 \times 10^{-4}$ Mwa/m² by the end of year 10.

5.1.2.3. International Thermonuclear Experimental Reactor. ITER (<http://www.iter.eu.de/>) is a moderate-field (5.3 T) burning plasma and technology development experiment based upon 5K niobium-tin superconducting TF and PF magnets, with actively cooled in-vessel PFCs and vacuum-vessel. Nominal operation is targeted towards 400-s $Q = 10$ DT burn with fusion power of 500 MW, sustained and controlled with NBI + ICRF + ECRF heating of up to 73 MW. All systems except the PF inductive drive capability are steady state capable, and the TF and PF magnets allow the possibility of longer-pulse, full-B and full- P_{fus} operation in “standard”, “hybrid extended-pulse” and “advanced tokamak/steady state” modes. A comprehensive physics development and optimization and “reactor-relevant” technology study/test program is planned. The first ten years of operation, summarized in Table 5–4 and Fig. 5–1, focuses on device and facility commissioning, physics studies and modest-fluence breeding blanket module tests. A follow-on 10-year technology-test phase would focus on concerted fluence accumulation for blanket module testing and development.

**Table 5-3
Ignitor 10-Year Operation Plan Summary**

Year	Total Pulses	HH Pulses	DD Pulses	95%D-5%T Pulses	DT Pulses	Neutron Yield (10 ²²)
1	4800	4800	0	0	0	0.0
2	2300	2150	150	0	0	0.0
3	1975	0	1925	50	0	0.0
4	1970	0	1700	270	0	0.1
5	1950	0	1580	270	100	0.7
6	1950	0	1400	350	200	2.0
7	1950	0	1350	400	250	3.0
8	1950	0	1200	400	350	5.0
9	1950	0	1150	430	420	7.0
10	1950	0	1100	400	450	9.7
Total	22745	6950	10555	2970	1770	9.7

**Table 5-4
ITER Operation Plan Summary**

Year	Phase/Species	Pulses	FPE Pulses	Cumulative FW Fluence (MWa/m ²)
1	H	1000	0	0.000
2	H	2000	0	0.000
3	H	2000	0	0.000
4	DD and D+T	2000	1	0.000
5	DT	2000	800	0.050
6	DT	1000	1000	0.130
7	DT	2000	1500	0.025
8	HD/LP DT	2000	2500	0.047
9	HD/LP DT	2000	3000	0.070
10	HD/LP DT	<u>2000</u>	<u>3000</u>	0.094
Total		18000	11800	0.094

5.1.3. In-Vessel Tritium Retention Issues

In-vessel retention of tritium (T) can have a potentially significant impact on the duration of operation (cumulative number of DT burn pulses) that can be conducted before action to remove/recover in-vessel inventory is required. The retention problem and resulting

operation constraints are particularly acute in a large-scale long-pulse facility such as ITER where kg-level quantities of T are involved.

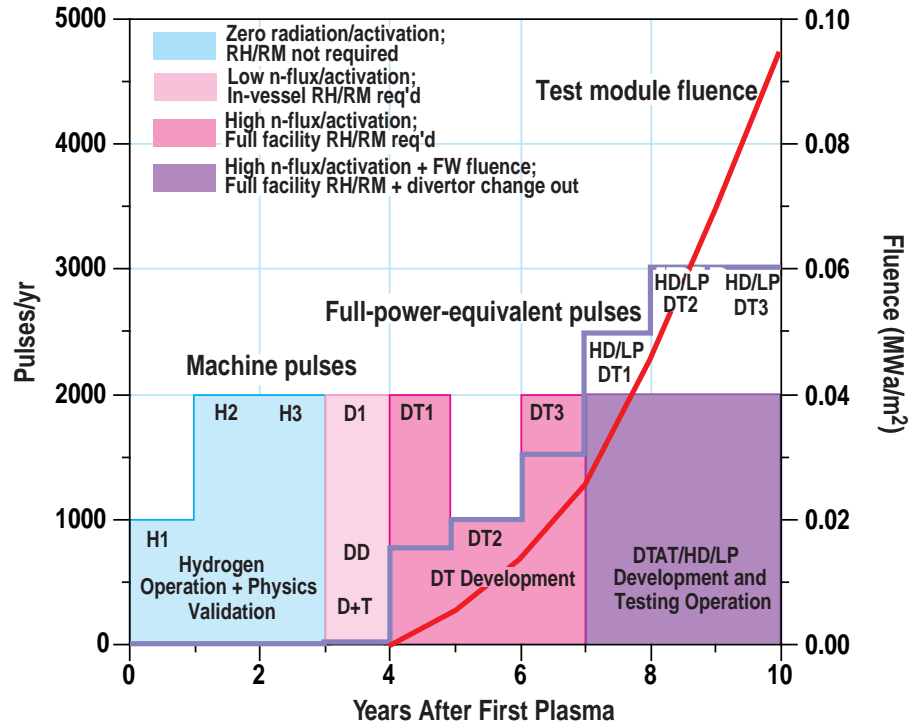


Fig. 5-1. ITER plan and cumulative FW fluence ($1 \text{ MWa/m}^2 = 3.15 \times 10^7 \text{ MJ/m}^2 = 1.39 \times 10^{25} \text{ n/m}^2$). Initial 10-year campaign.

Actual tritium burn-up on a per pulse (full power equivalent or FPE) basis is modest for all candidate machines: 6 mg for FIRE, 0.7 mg for Ignitor and 400 mg for ITER. Burn-up fraction (burned/initial fill) in one FPE pulse for FIRE and Ignitor is small: 8% and 3%. The ITER burn-up fraction is about 90%, but this high fraction and the lesser FIRE burn-up fraction are both achieved with plasma fueling (gas and/or pellet) rates that are 100 to 500 times the burn-up rates (e.g., FIRE once-through fueling is 0.7 g per FPE pulse; ITER once-through fueling estimate is 240 g per FPE pulse).

The key operation issue here is in-vessel retention of T, especially in a BPX with carbon PFCs. Plasma operation with such PFCs can will give rise to trapping of D and T in co-deposited carbon layers on and behind PFC surfaces. Extrapolation of present D and/or T co-deposition data to a large long-pulse carbon-bearing BPX like ITER suggests that retained T might be up to 1% to 10% of the injected fuel, so ~2 to 20 g might become entrained in co-deposited layers. While there is debate and uncertainty about the magnitude of the entrained fraction, even low retention fractions (say 1%, or 2 g per FPE pulse) will lead to significant in-vessel T for an ITER-class experiment, where the present “safety-based” design guideline specifies a 0.35 kg limit on in-vessel T.

The magnitude of the retention problem is much less for FIRE, where a 1% of fueling retention fraction would give about 7 mg per FPE pulse or 1.5 g per 200 FPE pulse operation year. This lesser retention is to be compared with an in-vessel limit (guideline) of 15 g. Furthermore, expected retention in an all-metal system is likely significantly less than 1%.

Similarly, small retention estimates apply for Ignitor, where the working assumption seems to be that the recycle rate for DT will be near unity and that only modest external fueling will be needed. In any case, the potential for substantial (on the 10-g scale) retained in-vessel T is small.

Both FIRE and Ignitor propose all-metal vessels and PFCs: first wall (FW) and divertor or limiter. FIRE proposes Be-surfaced tiles for the FW and W-surfaced PFCs and baffles for the divertor. Ignitor proposes a Mo-tile FW and limiter. Consequently, long-term retention of H/D/T is expected to be low. ITER proposes a mixed PFC material system, with Be-surfaced FW tiles, W-surfaced divertor baffles and secondary divertor PFCs and carbon-faced divertor high-heat-flux surfaces, so the source of carbon needed for significant in-vessel co-deposition will be present. ITER team estimates of the resulting expected overall in-vessel T retention are 1.5% of fueling, or about 4 g, per FPE pulse. On this basis, the in-vessel working limit will be reached in approximately 100 FPE pulses (~1 week of operation).

Table 5-5 summarizes the comparative operational impact of moderate (1% per FPE pulse) and low (0.1% per FPE pulse) retention in the three BPXs.

Table 5-5
Estimated In-Vessel T Retention and FPEs to Reach In-Vessel Limit

BPX	Ignitor	FIRE	ITER
FPE basis	100 MW x 4 s	150 MW x 20 s	500 MW x 440 s
T burnup per FPE (g)	0.0007	0.0055	0.40
Fueling per FPE pulse (g)	0.08	0.7	240
Allowable in-vessel T (g)	10 (?)	15	350
Retained T (g) per FPE, @1% of fueling retention	0.0008	0.007	2.4
FPEs to reach limit	12,500	2,150	146
FPE/yr	100	200	2,000
Years to limit	125	10.8	0.073
Years to limit (0.1% retention)	1250	108	0.73

Discussion of the many scientific and technical aspects of T retention in metals and carbon and how such tritium can be removed and recovered during operation is beyond the scope of the E3 charter. Here it suffices to note that if per-fueling-pulse retention levels with all-metal systems are in the $\leq 1\%$ range, FIRE and Ignitor will encounter little to no

appreciable operational or tritium supply constraints owing to such retention. ITER, on the other hand, will encounter a T-retention problem within less than 1 month of sustained full-FPE operation (<200 FPE pulses) at the 1%-of-fueling retention level. Even with presently projected “all-metal” retention levels (~0.1%), action to remove in-vessel-retained T in ITER will have to be taken on an annual basis. Whether or not such annual removal will impose a further constraint (not already provided in the draft ITER operation schedule) on the scheduled annual availability is a matter for future ITER team and tritium-recovery expert consideration.

5.2. ENGINEERING

The Fusion Ignition Research Experiment (FIRE) is being studied as a possible Next Step Option in the U.S. fusion program. The purpose of the Engineering task is to provide engineering management and technical input for FIRE and other systems (e.g., ITER). This is a continuing effort performed by R.J. Thome of GA as Engineering Manager for NSO FIRE. Physics Management for FIRE is done by D. Meade (PPPL) and overall Management by J. Schmidt (PPPL). FIRE engineering Reports were issued in FY99, FY00 and FY01. The latter was updated for use at the 2002 Fusion Summer Study at Snowmass. This material, as well as other related items, is available on the PPPL web site at <http://fire.pppl.gov>.

The FIRE preconceptual design involves pulsed, liquid nitrogen cooled, copper toroidal and poloidal field coils. A configuration with wedged TF coils and a free-standing central solenoid was selected in FY02. The wedged option allows fields of 10 T to be achieved for pulse lengths of about 20 s with a plasma current of 7.7 MA, but requires the inboard legs of the TF coils to use BeCu. The design is evolving toward more emphasis on AT modes (6.5 T, 5 MA, 150–200 MW). Cooling has been added to both sides of the inboard leg of the TF coils so that cooldown following a full power pulse requires slightly more than 1 h. The trend, to be confirmed in FY03 analyses, is toward a machine with a major radius of 2.14 m and a minor radius of 0.595 m.

The engineering aspects of FIRE were summarized in two papers in FY02:

- P.J. Heitzenroeder and R.J. Thome, “Engineering Status and Plans for the Fusion Ignition Research Experiment (FIRE),” 19th SOFE, Atlantic City, New Jersey, January 2002.
- R.J. Thome and P.J. Heitzenroeder, “Engineering Overview of the Fusion Ignition Research Experiment (FIRE),” ISFNT6, San Diego, California, April 2002.

Figure 5–2 shows key features of the FIRE baseline design.

- 16 wedged TF coils
- Two pairs of external divertor coils
- Two pairs of external ring coils
- Free-standing, segmented central solenoid
- Vacuum vessel filled with steel/water for shielding
- Plasma facing components:
 - Be coated Cu first wall
 - W pin-type inner divertor, baffle and out divertor

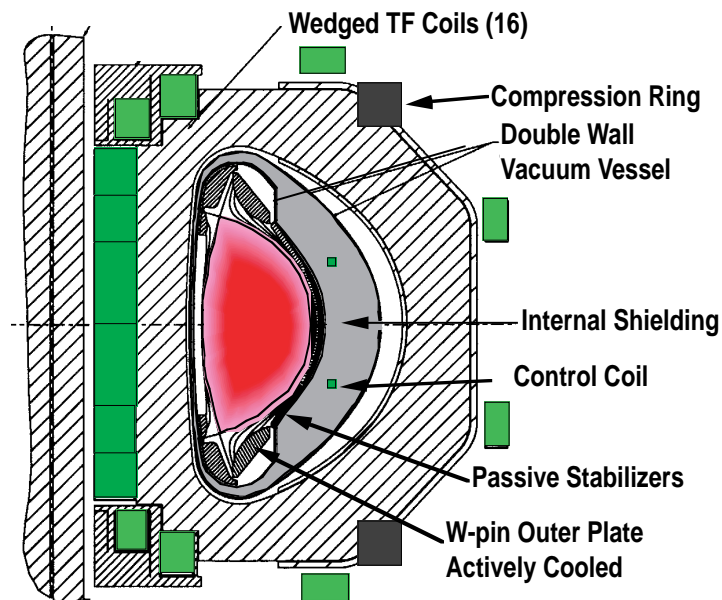


Fig. 5–2. Features of FIRE baseline.

- Two outboard poloidal limiters
- Internal passive and active stabilization coils
- Remote maintenance
- 16 large midplane ports
- 32 angled ports
- 32 vertical ports

- Thermal shield
 - SS frame with SS skin
 - Insulated exterior
 - Provides 80–90 K inside

Late in FY02, technical discussions began concerning the ITER Central Solenoid (CS). The ITER CS will be a large scale, state-of-the-art, high field (13 T), pulsed superconducting magnet system. It will be composed of six 110 ton modules that could be supplied by the U.S. to contribute to the fusion program and superconducting magnet technology development in U.S. industry. The CS will use advanced Nb₃Sn superconductor, high nickel steel jacket for the conductor, and complex fabrication techniques requiring advanced tooling and procedures. The features of the CS are summarized in Table 5–6.

The U.S. supplied a close to full scale 13 T module as part of the ITER EDA. It has been successfully operated in a pulsed mode in a facility in Japan as part of a two-year test program.

Table 5–6
Features of the ITER Central Solenoid

Central Solenoid	Winding configuration	6 modules
	Overall coil height (excluding structures)	12.1 m
	Overall coil outer diameter	4.15 m
	Overall weight (including structures)	840 ton
Module (1 of 6)	Inner diameter	2.6 m
	Outer diameter	4.15 m
	Height	2 m
	Module Weight	110 ton
	Conductor unit length	812 m
	Total conductor length	5682 m

5.3. THERMAL ANALYSIS OF FIRE DIVERTOR

A thermal analysis of the FIRE divertor was performed in three parts: stress (Section 5.3.1), hydraulic (Section 5.3.2), and fatigue (Section 5.3.3).

5.3.1. Thermal Stress Analysis

A 3D thermal stress analysis of a segment of the FIRE divertor was performed using a finite element model input to the COSMOS code [5–1]. The heat flux distribution on the surface of the tungsten brush was modeled. Since only 20 cm of the divertor of the total

length of 55 cm is subjected to the high heat flux, only a 20.4 length is modeled. It is assumed that the pins slanted at 30 deg though the lower portion of the model provides zero displacements in the three principal directions (i.e., a rigid backing plate at 20°C is assumed). The support pins are spaced every 1.2 cm along the length of the divertor segment and assumed to be made from 316 LN stainless steel. The resultant reaction loads at the support locations are used to calculate the shear stress in the pins.

It is assumed that the divertor segment is free from residual stresses due to fabrication. The top of the coolant channels are positioned 3 mm below the melt zone material consisting of the tungsten copper joint. A study of the impact of flow direction on coolant temperature at the location of highest heat flux indicated that the flow direction did not make a significant difference. Hence, an inlet at high heat flux end, suitable for manifolding, was chosen. The coolant temperature varies from 30°C to 95°C along the channel. The convection film coefficient varies as a function of film temperature (average of coolant channel surface and coolant) and was calculated by correlations developed for ITER [5-2,5-3,5-4]. The material property data was assigned as a function of temperature [5-5,5-6].

5.3.2. Thermal Hydraulic Analysis Results

In order to remove an incident peak heat flux of 25 MW/m², a very large flow velocity (>20 m/s) is required if smooth channels are used. The flow velocity and flow rate required to cool the divertor can be reduced by using a heat transfer enhancement in the flow channels. A review of enhancement methods [5-7] shows that a swirl tube (ST) is the best available method. The ST is easy to fabricate and has a large reliable database. For a ST with a tape thickness of 1.5 mm and a twist ratio of 2 in the divertor channels of 8 mm diameter, a flow velocity of 10 m/s gives sufficient safety margin on CHF for the divertor. If two adjacent channels are connected in series, the maximum outlet temperature is 95°C and minimum exit pressure is 1.05 MPa, resulting in a minimum subcooling of 87°C.

A two dimensional finite element analysis of a divertor cell has been previously performed for these flow conditions [5-7]. This analysis was refined by a 3-D model. The divertor cell consists of two copper mono blocks with the 5 mm tungsten brush as PFC. An effective thermal conductance of the tungsten copper interphase was previously determined by a 3 D finite element analysis [5-7]. The heat transfer coefficient in the coolant channel is calculated as function of film temperature over forced convection and nucleate boiling region [5-7,5-8]. The pressure drop is calculated by Lopina-Bergles correlation [5-8].

A steady state condition is reached in about 6 s. The peak surface temperature is 1362°C and the peak heat flux on the coolant channel wall (WHF) is 29.75 MW/m². Since the calculated wall critical heat flux under these conditions is 48 MW/m² (this CHF value is much higher than calculated for ITER due to much lower coolant temperature for FIRE), we

have a safety margin of about 1.61. The maximum copper temperature is 406°C. The flow per module is 9 l/s. The thermal hydraulic results are summarized in Table 5–7.

**Table 5–7
Results of Thermal Hydraulic Analysis**

Parameter	Outer Divertor
Peak heat flux (MW/m ²)	25
Maximum PFC temperature (°C)	1362
Maximum copper Temperature (°C)	406
Flow velocity (m/s)	10
Flow/module (l/s)	9
Exit coolant temperature (°C)	95
Exit pressure (MPa)	1.06
Exit subcooling (°C)	87
Wall CHF (MW/m ²)	48.
Maximum wall heat flux (MW/m ²)	29.75

5.3.3. Thermal Fatigue Analysis of FIRE Divertor Segment

An elastic-plastic thermal fatigue stress analysis of the FIRE divertor segment was completed using the structural model and thermal loading [5–9]. The results of Ref. 9 showed that the maximum Von Mises thermal stress in the heat sink exceeds the $3S_m$ allowable value specified in Ref. 6. Therefore, an elastic-plastic stress analysis was performed to calculate the strain-controlled fatigue life of the Cu-Cr-Zr heat sink for repeated heat-up and cool-down cycles.

The thermal loading specified in Ref. 9 is input as a transient over a heatup and cooldown cycle to calculate the maximum total strain range in the heat sink. The calculated total strain range for the first heatup and cooldown cycle is used to determine the number of cycles to failure from the strain controlled fatigue data given in Ref. 5 for unirradiated Cu-Cr-Zr material over the temperature range of 20°C to 350°C.

The maximum total strain in the heat sink occurs on the top surface above the coolant holes and away from stress concentrations. The peak steady state temperature at this location is 405°C which produces a compressive total effective strain of 0.447%. During cooldown, the maximum effective tensile strain on the top surface of the heat sink is 0.143%. The fully reversed strain range is therefore just under 0.30%. The strain fatigue curve from Ref. 5 predicts that 10,000 fully reversed cycles are required to produce fatigue failure in the heat sink. This provides a safety factor of 3.3 on the number thermal cycles specified for the divertor design. It is to be noted that the analysis was performed using unirradiated material

properties for Cu-Cr-Zr and that data for Young's modulus and strain controlled fatigue curves are needed to evaluate the heat sink in its expected irradiated state.

The elastic-plastic stress analysis of the divertor requires that the thermal analysis be executed as a transient analysis so that the thermal loads are applied in incremental time steps. A pseudo time curve is used to apply the thermal loads in steps so that yielding of the heat sink can be incrementally calculated. The heat flux distribution along the length of the divertor described in Ref. 9 is input according to the following time steps shown in Table 5-8.

A peak temperature of 405°C on the top surface is attained after a hold time of 6 s. Cooldown to 60°C is achieved at the end of the 15-s loading curve.

Table 5-8
Flux Distribution Time Curve

Time (s)	Multiplying Factor
0	0.0
2	1.0
8	1.0
10	0.0
15	0.0

The non-linear thermal stress analysis was performed using the COSMOS code. The boundary conditions input to the structural model assume that the support pins permit thermal expansion of the heat sink in the axial direction, but not in the vertical direction. The values used for the temperature dependent material properties for unirradiated Cu-Cr-Zr [5] are shown in Table 5-9.

Table 5-9
**Temperature Dependent Material Properties
for Unirradiated Cu-Cr-Zr**

T (°C)	E×10⁶ (n/cm²)	α×10⁻⁶ (°C)	σ_y×10³ (n/cm²)	E_{TAN}×10³ (n/cm²)
20	12.8	15.7	29.7	100
300	11.5	17.6	24.6	80
400	10.9	18.2	22.2	60
500	10.2	18.6	19.4	40

The maximum effective total strain is 0.447% and is compressive. At the end of the first cooldown cycle, the total effective tensile strain is 0.143%. The plastic strain distribution at

the end of cooldown shows that about a 4.0 cm length of the divertor segment will retain residual stresses. Subsequent thermal cycles will result in strain cycling between these values in the plastic regime. The total strain range used for estimating the number of cycles to failure as determined from fully reversed ($R = -1$) controlled strain fatigue data is 0.30%. The number of cycles to failure at 0.30% strain range is seen to be 10,000 from strain controlled fatigue curve for unirradiated Cu-Cr-Zr over a temperature range of 20°C to 350°C [5–5]. This provides a safety factor of 3.3 on the specified number of operational cycles. A fatigue evaluation of the divertor using irradiated material properties and fatigue data should be performed when all data for irradiated Cu-Cr-Zr is available.

References for Section 5

- [5–1] COSMOS, A Finite Element Analysis Code, Structural Research, Santa Monica, California.
- [5–2] M. Araki et al., “Data Bases for Thermo Hydraulic Coupling with Coolants, Atomic and Plasma-Material Interaction Data for Fusion,” Supplement to the J. Nucl. Fusion, **5** (1994).
- [5–3] J. Schlosser et al., “Thermal Hydraulic Testing for ITER High Heat Flux Components,” SOFT-20, pp. 137-140.
- [5–4] C. B. Baxi, “Thermal Hydraulics of Water Cooled Divertors,” presented at the SOFT-21, Madrid, Spain, 2000.
- [5–5] ITER Material Properties Handbook, ITER Document No. S 74 MA2.
- [5–6] ITER Interim Structural Design Criteria, S 74RE2 96-06-18 W1.1, Appendix A, p. 33.
- [5–7] C. B. Baxi, “Thermal Analysis of FIRE Divertor and Baffle,” Presented at ANS Topical Meeting, Park City, 2001.
- [5–8] R.F. Lopina and A.E. Bergles, “Heat Transfer in and Pressure Drop in Tape Generated Swirl Flow of Water,” J. Heat Transfer, **91**, 434 (1969).
- [5–9] C.B. Baxi et al., “Thermal Stress Analysis of FIRE Divertor,” Presented at 22nd SOFT, Helsinki, Finland, 2002.

6. ADVANCED LIQUID PLASMA SURFACE (ALPS)

We completed the grid structure for the MCI calculation of the lithium transport from DiMES, including the plasma background from B2.5/UEDGE codes and lithium emission from the WBC code. This is the first complete coupling with these codes. Initial MHD modeling results showed the possibility of getting the lithium injected vertically to the plasma core at a speed of ~20 m/s, but the necessary current density would be 3–4 time higher than that estimated from a 2-D calculation. Preliminary MCI lithium transport results from a DIII–D low power Li shot, with the outer strike point positioned on the center of the DiMES Li sample, showed a significant amount of core Li penetration. In contrast to carbon, we found that lithium tends to enter the core in a relatively low charge state and spreads rapidly into the far SOL region.

6.1. MODELING

We completed the grid structure for the MCI calculation of the lithium transport from the lower divertor of DIII–D (DiMES-location), including the plasma background from B2.5/UEDGE and lithium emission from the WBC code. This is the first complete coupling with these codes. Preliminary runs were attempted using the Li initial conditions provided by the WBC code from ANL. Results on Li transport from the DIII–D Li DiMES experiment have been obtained using a new impurity source module in the MCI code. The new module worked very well and produced results that suggest some of the sputtered Li entered the core (possible in the vicinity of the x-point). This simulation was run with a background plasma solution from B2.5 and a WBC sputtering distribution. In contrast to carbon, we found that lithium tends to enter the core in a relatively low charge state and spread rapidly into the far SOL region. We observed singly ionized Li entering the core just below the outer mid-plane and a rather large flux of Li^{1+} redeposited on the target plates near both the inner and outer strike points. Li^{2+} was found relatively far out in the SOL above the x-point on both the low field side (outboard) and the high field side (inboard) but appeared to recombine rapidly (to Li^{1+}) as it moved into the high field side divertor region. On the low field side, Li^{2+} survived all the way down to the target plates in a narrow channel located about 10–12 cm outside the outer strike point. The only atomic lithium found for this discharge condition was located in the private flux region and its concentration levels were very small.

6.2. LI MHD MODELING AND ANALYSIS

Neil Morley of UCLA presented an initial MHD modeling result of the Li-DiMES disruption experiment. He showed the possibility of vertical injection of lithium at a speed of ~20 m/s, but the 2-D model shows that the current density would be 4–5 times higher than could be provided by the parallel current. This could still be credible with the reduction in current flow area for the actual 3-D geometry of the liquid lithium. Additional current could be contributed from unipolar arcing.

Evans of GA analyzed the Li-DiMES disruption experiment. He found that current density across the Li surface is non-uniform and suggested that this should be modeled to determine if this could be the cause of radial lithium injection. He also found that during a discharge the scrapeoff layer current could change sign during an ELMing event; this could create an additional challenge for the use of lithium at the divertor.

6.3. LI-DIMES EXPERIMENT

Further analysis of the Li-DiMES data on lithium sputtering was performed and a paper was prepared for Nuclear Fusion. With incident D⁺ energy ~100 eV, the physical sputtering yield of liquid phase lithium near the melting point is ~0.05 atoms/ion. Measured solid lithium erosion yields from DiMES under quiescent conditions agree well with laboratory data scaled from plasma and ion beam facilities. The data indicated that lithium has acceptably small effective sputtering yields for application as a plasma-facing component in the tokamak.

6.4. ATOMIC DATA

We were contacted by Dr. Stuart Loch, Physics Department at Auburn University, who is involved in an Atomic Data and Analysis Structure (ADAS) group effort to produce a comprehensive atomic data set for all iso-nuclear stages of lithium. This data will ultimately become part of the standard ADAS distribution. Dr. Loch wanted additional details on what data is needed and how it will be used. The goal of the project is to generate electron excitation data (using R-Matrix) for all ionization stages of lithium along with dielectronic recombination and ionization data for all stages. In addition, they will be working on high quality time dependant calculations for a couple of transitions for all ionization stages. We requested that they include the most up-to-date charge exchange cross-sections and emission rates. This data is particularly important for lithium transport modeling and will be useful for Li beam diagnostic analysis.

6.5. CONFERENCES/MEETINGS

1. Whyte and Wong attended and made presentations at the ALPS project meeting.
2. Evans presented a talk on “Modeling and diagnostic needs of specific interest for advanced tokamak scenarios,” at the 1st IAEA Coordinated Research Meeting on Atomic Data Needs for Tokamak Diagnostics in Vienna, Austria on November 12–13.
3. Evans made a presentation on “DIII–D Atomic Data Related Activities” for the ADAS Atomic Database Workshop in Cadarache, France, 20-22 of October. He also participated in the ADAS Atomic Database Steering Committee Meeting following the workshop.

7. ADVANCED POWER EXTRACTION STUDY (APEX)

We coordinated the APEX Task IV: the solid first wall and blanket design task. Wong visited JFT-2M at JAERI and learned about the positive experimental results of the magnetic field ripple reduction with ferritic steel (FS) inserts. Subsequently, we initiated the study of nano-composite ferritic steel (AFS) and Flibe-cooled FW/blanket design. A reference AFS/Flibe FW/blanket design with recirculating coolant routing was selected as the reference solid wall APEX design.

7.1. SiC_f/SiC DESIGN ASSESSMENT

For the SiC_f/SiC composite material assessment, using the finite elements ANSYS code, Shatoff of GA generated the first single-fiber model structural response results, which match quite well with the results from experimental measurement of single-fiber pushout tests. We also completed the coordination on the assessment of the SiC_f/SiC-LiPb design concept. Our results confirmed those generated by the ARIES-AT design. But due to the lack of materials data on radiation damage, the credibility of SiC_f/SiC as the fusion reactor structural material is still uncertain.

7.2. FERRITIC STEEL DESIGN

We proposed new tasks on the assessment of ferritic steel and Flibe as the structural and breeding material, respectively, as the solid first wall and blanket design. During preliminary assessment, we found that due to the change of saturation magnetic field as a function of temperature, 10% spatial variation of magnetic field strength could result from the thermal distribution of the first wall blanket design. Wong visited JFT-2M at JAERI and learned about the positive experimental results of magnetic field ripple reduction with FS inserts. Their second experiment with toroidal rings of FS in the plasma chamber showed no adverse effect to plasma operation and confinement. Their third experiment with the plasma chamber covered completely with FS plates is expected to reduce the field ripple to ~0.3%.

7.3. AFS/FLIBE FIRST WALL AND BLANKET DESIGN

We coordinated the development of AFS and Flibe cooled first wall concept. Technical guidelines were developed and distributed for concept comparison. Four different concepts, one from FZK, two from the University of Wisconsin, and one from GA were proposed.

GA completed the assessment of the concept using helical channels wrapped around a poloidal geometry blanket module. High neutron wall loading (5 MW/m^2) and the corresponding heat flux removal can be accommodated within material temperature limits by proper design. However, the system has a relatively high pressure drop of $>4 \text{ MPa}$. A new integrated once-through poloidal flow first wall design was conceived and assessed. The system pressure drop is reduced to $\sim 1 \text{ MPa}$, and the tritium breeding performance also improved. This concept was used to compete with the three other concepts.

We coordinated the selection of the reference FW/blanket design. Four solid first wall blanket concepts were evaluated. They are the helical Be-multiplier concept, the helical first wall flow concept, the once-through flow concept and the recirculating flow concept. The last two concepts are very similar in coolant routing and thermal performance. The APEX Task IV team selected the recirculating coolant concept, which allows easier drainage of the high melting point Flibe when necessary during maintenance and accident conditions, and allows control of the first wall cooling with the use of the recirculating pump.

7.4. THERMAL HYDRAULICS ASSESSMENT

A design evaluation was performed to define the parameters for the reference AFS/FLiBe FW/blanket design. This consists of a systems study to determine the reactor embodiment of the blanket module and the corresponding neutron and surface heat flux wall loadings. The key design temperature limitations for the combined use of AFS as structural material, FLiBe as the tritium breeder and coolant, and Pb as the neutron multiplier are:

Maximum temperature limit for AFS	800°C
Maximum temperature limit for AFS/FLiBe interface	700°C
Maximum temperature limit for AFS/Pb interface	700°C

The inboard and outboard FW/blanket modules of a tokamak reactor are shown in Fig. 7-1. The cross-section of the outboard FW/blanket module of the recirculating flow concept is also shown. The coolant flow routing is shown in Fig. 7-2. The FLiBe coolant enters the bottom of the blanket module from the FW/blanket mixer (stream A) and moves upward cooling the first wall. It turns around at the top of the poloidal module, splits into two streams flowing down the poloidal module. The first stream (the recirculating stream B) cools the side and back walls of the blanket, gets to the recirculating pump and then the FW/blanket mixer. In parallel, stream C cools the central zone of the FW/blanket module. The FW/blanket power is removed at the heat exchanger before the coolant stream returns to the pump as shown in Fig. 7-2. The two downward flowing streams are combined in the mixer before flowing up to cool the first wall again. The flow design parameters of these

coolant streams can be adjusted by changing the mass flow rate of the recirculating stream, which is controlled by the recirculating pump located at the bottom of the module as shown.

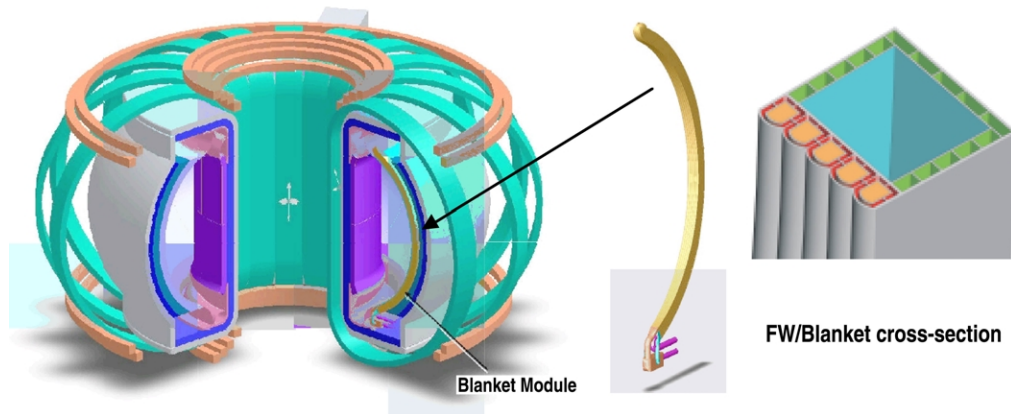


Fig. 7-1. APEX recirculating blanket tokamak reactor, poloidal module and FW/blanket cross-section.

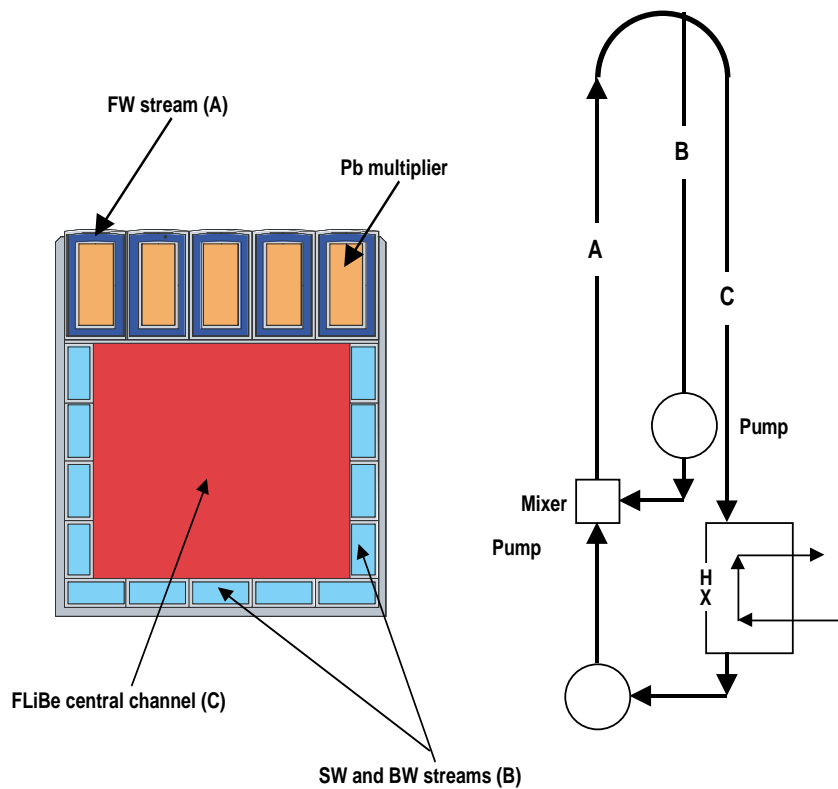


Fig. 7-2. FW/blanket cross-section and coolant routing.

For a 16 toroidal field coil tokamak reactor design, as shown in Fig. 7-1, there are 5 poloidal inboard modules and 9 poloidal outboard modules per sector. The inboard and outboard modules at the mid-plane have similar width of 0.3 m. Hydraulic dimensions of

these modules are also similar. It should be noted that this analysis assumes uniform flow cross-section of the FW/blanket module. For the reactor outboard there are front and back blankets. The back blanket picks up 3.7% of the total reactor thermal power.

For the thermal hydraulics assessment the following inputs and assumptions were used:

- Radial distributions of power density for the first wall, sidewalls, backwall, neutron multiplier and the FLiBe zones were obtained from neutronics calculations.
- Inboard and outboard FW/blanket designs were considered. Since the outboard back blanket intercepts only 3.7% of the total reactor thermal power, only the front outboard blanket design was considered in the analysis.
- To get the poloidal distribution of surface heat flux, 14.4% of the plasma core radiation is from Bremsstrahlung radiation and it has a poloidal power distribution. The remaining 85.6% is from line-radiation, which is distributed uniformly to the reactor chamber.

Results of the inboard and outboard reference design are shown in Table 7–1. We found that by adjusting the recirculation flow mass flow rate, the inboard temperatures can be adjusted to be similar to the outboard blanket temperatures, even though the outboard blanket is limited by the T_{\max} of AFS and the inboard design is limited by interface temperature between FLiBe and AFS, and the over all thermal performance is further constrained by the interface temperature limit between Pb and AFS. Without including the MHD effect, the inboard and outboard total pressure drops are 0.41 and 0.84 MPa, respectively.

Table 7–1
Thermal Hydraulics Parameters of the Inboard and Outboard FW/Blanket Modules

	Inboard	Outboard
Number of module per sector	5	9
Mid-plane module width, m	0.3	0.3
Input power per module:		
Module power, MW	8.7	13.2
First wall including heat flux, MW	5.8	6.9
Side+back wall, MW	0.88	1.45
Central Flibe column, MW	2.97	4.88
First wall and Pb zone at inlet/ mid-plane /outlet, of the outboard, unless specified:		
FW Heat flux, MW/m ²	0.73/ 0.86 /0.73	0.73/ 1 /0.73
Max. neutron wall loading, MW/m ²	1.9/ 3.6 /1.9	2.8/ 5.4 /2.8
Neutron poloidal peaking factor to chamber average	0.95	1.42
FW mass flow rate, kg/s	71.2	98.6
T _{coolant-bulk} , °C	585/ 602 /619	585/ 599 /614

Table 7-1 (Cont.)

	Inboard	Outboard
Flibe velocity, m/s	4.57/ 4.59 /4.61	6.33/ 6.36 /6.38
Hydraulic diameter, cm	1.54	1.54
Re	11,012/ 12,230 /13,529	15,259/ 16,698 /18,218
h, W/m ² K	9,264/ 9,866 /10,482	12,427/ 13,118 /13,821
FW NCF/Flibe T _{interface} , °C	669/ 699 /694	650/ 687 /673
FW T _{max} , °C	738/ 791 /763	720/ 799 /743
Pressure drop, MPa	0.41	0.74
Mid-plane Pb wall NCF/Flibe interface T, °C	625	633
Mid-plane Pb wall NCF/Pb interface T, °C	649	679
Mid-plane Pb max, °C	922	1186
Side and back wall at inlet/ mid-plane /outlet, unless specified:		
Mass flow rate, kg/s	51	68
T _{coolant-bulk} , °C	619/ 623 /626	614/ 619 /623
Mid-plane Flibe velocity, m/s	2.75	2.75
Hydraulic diameter, cm	2.61	2.61
Mid-plane Re	10,262	13,360
Mid-plane h, W/m ² K	4796	6125
Pressure drop, MPa	0.050	0.084
Central Flibe zone at inlet/mid-plane/outlet unless specified:		
Mass flow rate, kg/s	20.17	30.6
T _{coolant-bulk} , °C	619/ 650 /681	614/ 649 /681
Mid-plane Flibe velocity, m/s	0.22	0.33
Estimated residence time, s	36	24
Hydraulic diameter, cm	21.8	21.8
Mid-plane Re	10,490	15,734
Mid-plane h, W/m ² K	558	807
Pressure drop, MPa	0.000066	0.000137
Total module FW/blanket pressure drop, MPa	0.464	0.820

7.5. CONFERENCES/MEETINGS

1. Wong attended the 10 ICFRM meeting at Baden Baden, Germany.

2. Wong attended the JUPITER-II Flibe-task workshop in Tokyo, visited JFT-2M and completed the FY01 exchange on helium-cooled reactor components with the Reactor Design Group at JAERI, Naka, Japan.

7.6. PUBLICATIONS

1. C. Wong et al., “Advanced high performance solid wall blanket concepts” *Fusion Engineering and Design* **61–62** (2002) 283.
2. L. Barleon et al., “The Transpiration Cooled First Wall and Blanket Concept” *Fusion Engineering and Design* **61–62** (2002) 477.

8. PLASMA-FACING COMPONENTS — DiMES

We repaired the hydraulic pump of the Divertor Materials Evaluation System (DiMES) and performed a very successful in situ heat flux measurement experiment with the embedded diagnostics wires. We studied plasma wall interaction issues and found that the main-wall neutral recycling, as measured by D_{α} , is correlated to local plasma main-wall flux regardless of confinement regime. We successfully carried out the first disruption detection and mitigation experiment with a massive injection of neon gas. We completed the analysis on the high net erosion rate of carbon with neon-detached plasma. A likely cause of the high net carbon erosion rate is physical sputtering by neon and chemical enhancement by the formation of hydrocarbons. We also completed the assessment on the Smart Tile concept and the initial proposal was sent to Virtual Laboratory for Technology (VLT).

8.1. DiMES MECHANISM

Corrosion residue from the internal phone cord holding the instrument cables was found in the hydraulic fluid of the DiMES sample transfer system and caused a failure of the hydraulic pump. After getting approval from the DIII-D vacuum committee, we replaced the pump and we also selected to use a less expensive hydraulic fluid, which has a higher vapor pressure than the very expensive hydraulic fluid that we had been using. Another advantage of the new fluid is that it can be operated at room temperature, while the old fluid needed to operate at an elevated temperature.

The instrument cables were tested and found to be acceptable. This allowed us to continue our experiments. A small team of engineers was assembled to replace the instrumentation cable during the major vent in October 2002. A new fixture was fabricated to hold the DiMES vertical bellows in place for the efficient removal of the DiMES sample changer while maintaining vertical alignment.

8.2. DIII-D EXPERIMENTS

A very successful in situ heat flux measurement experiment was performed with the embedded diagnostics wires in DiMES. J. Watkins of Sandia National Laboratory designed the instrumented sample and performed the experiment. The variation of divertor surface temperatures was measured as a function of time when the plasma strike point was scanned across the lower divertor.

The first experiment was carried out to detect and mitigate in real-time DIII–D disruption-caused damage. Vertical and thermal instabilities were successfully detected by the plasma-control system and a massive injection of high-pressure neon gas jet safely terminated the plasma in ~5 ms. Control room analysis indicated better thermal and halo current mitigation of the vertically unstable plasma when the threshold for gas jet triggering was set at a small value (~1–2 cm) away from the equilibrium position.

The Sandia designed W-rod DiMES sample was received. The sample was baked under the standard procedure at GA and it was ready to be exposed as a piggyback experiment to study the heat flux distribution on the W-rod surface.

8.3. EXPERIMENT IN C–MOD

We proposed an experiment to the Alcator-C Ideas Forum that would measure the particle balance, wall pumping and global fuel retention rate on the all-metal C–Mod tokamak. Results from this experiment would be compared to companion experiments on the graphite DIII–D tokamak.

8.4. CHAMBER RECYCLING

It was shown that the main-wall neutral recycling, as measured by D_{α} , is correlated to local plasma main-wall flux regardless of confinement regime. This strongly supports the concept of main-chamber recycling on DIII–D. A Langmuir probe embedded in the upper divertor knee was used to diagnose plasma flux to this axisymmetric surface with lower single null plasmas. The knee acts as a belt-limiter and was positioned in the far SOL at 9 cm flux surface (mid-plane equivalent). It was found that the local D_{α} induced neutral flux matched plasma flux in magnitude and trend through L–mode, ELM-free H–mode, ELMy H–mode and during the ELMs themselves, despite the order of magnitude changes occurring in recycling among these different regimes. This further emphasizes the important role ELMs play in recycling during H–mode since the main-wall plasma flux/recycling increased a factor of 10 during the ELMs despite the large distance of the probe from the close flux surfaces.

8.5. ANALYSIS OF Ne INJECTION DETACHMENT

Bill Wampler of Sandia National Laboratory analyzed the measurements of erosion of divertor materials by a detached plasma formed by neon injection. Neon injection cooled the plasma edge by radiation, reduced the temperature and increased the density of the divertor plasma, and reduced the peak heat flux onto the divertor plate, while maintaining good H–mode energy confinement and purity of core plasma. However, the rate of carbon erosion by neon-detached plasma is very high, 15 nm/s, in contrast to the absence of erosion by

plasma detached by deuterium injection. Figure 8–1 shows the net carbon erosion along a line in the radial direction passing through the center of the probe. The erosion peaks near the location of the separatrix has a value of 250 nm.

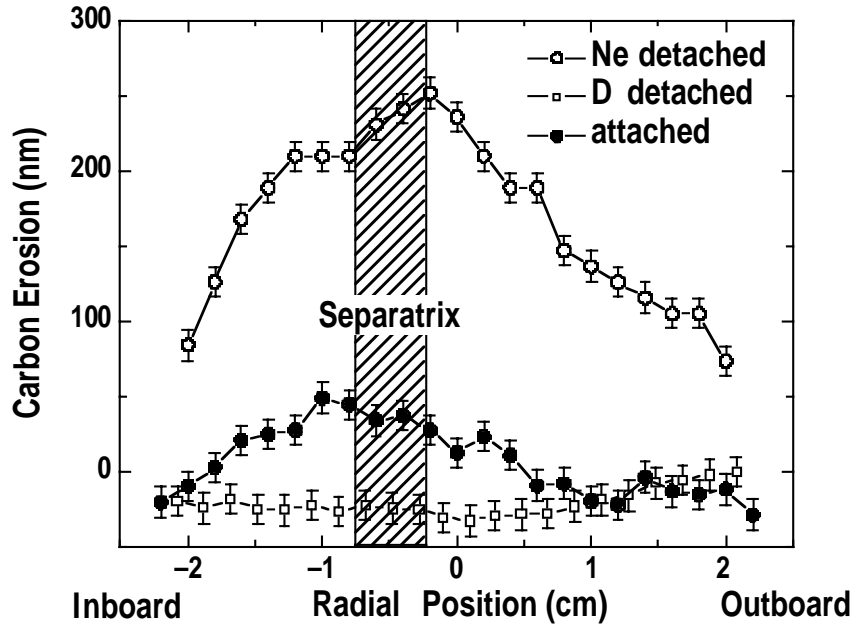


Fig. 8–1. Measured net carbon erosion along a line in the radial direction. The shaded region indicates the location of the OSP separatrix. Negative values correspond to net deposition. Open dots for neon detached plasma 17 s exposure, solid dots for deuterium attached plasma 13 s exposure, open squares for deuterium detached plasma 18 s exposure.

For comparison, Fig. 8–1 also shows the net carbon erosion and deposition measured previously along the same line on similar samples, exposure at the outer strike point (OSP) for 18 s to plasma detached by deuterium injection, and exposure for 13 s to attached plasma.

A likely cause of the high net carbon erosion is sputtering by neon. The kinetic energy of ions striking the surface should be the thermal energy ($\sim kT_i$) plus the energy gained by acceleration through the sheath ($\sim 3ZkT_e$), plus energy due to plasma flow. The energy due to plasma flow is $M_{Ne}/M_D kT_i = 10 kT_i$, for neon in a primarily D plasma flowing at the sound speed. The plasma should be close to thermal equilibrium ($T_i \sim T_e$). The average charge state (Z) of neon ions should be close to one for low temperature detached plasma. The energy of neon ions striking the divertor should therefore be $E_{Ne} \sim 14 kT_e$, predominantly due to the plasma flow. This gives neon energies in the range from 20 to 50 eV for the lower temperature plasma state ($T_e = 1.5$ to 4 eV), and in the range from 175 to 350 eV for the higher temperature plasma state ($T_e = 12$ to 25 eV).

Yields for physical sputtering of carbon by neon at normal incidence are 0.1 to 0.2 C/Ne for energies corresponding to the higher temperature state, and are predicted to be very small

for the low temperature state for which the ion energy is below the threshold (70 eV) for sputtering. However, sputtering yields on a carbon divertor are likely to be higher than these values, particularly at low energies, for two reasons. First, neon ions strike the divertor surface at oblique angles of incidence, which results in lower threshold energies and higher sputtering yields. Secondly, the high flux of deuterium onto the divertor forms hydrocarbons, which are less strongly bound than atomic carbon. Kinetic ejection of hydrocarbon complexes from the surface by collisional energy transfer results in much higher effective sputtering yields at low energies. Threshold energies for sputtering by this process are estimated to be only 1 or 2 eV instead of 70 eV for neon at normal incidence on carbon. These two effects might result in carbon sputtering yields of order unity for neon from the higher temperature plasma state and possibly also high sputtering yields for the lower temperature state.

The flux of neon required to produce the observed rate of carbon erosion ($\Gamma = 15 \text{ nm/s}$) is $\Phi_{\text{Ne}} = \Gamma N_{\text{C}}/Y = 1.5 \times 10^{21}/\text{m}^2\text{s}$, where $N_{\text{C}} = 10^{29}/\text{m}^3$ is the atomic density of carbon and using a sputtering yield of $Y = 1 \text{ C/Ne}$. The average ion flux onto the OSP, measured by a Langmuir probe, was about $10^{23}/\text{m}^2\text{s}$. Thus, a neon flux of 1.5% of the total ion flux could produce the observed carbon erosion, assuming a sputtering yield of one during the entire exposure and no carbon redeposition. If sputtering occurs only during exposure to the high temperature state, the effective exposure is about 25% of the time and the neon flux would need to be 6% of the total ion flux to give the observed erosion rate. These fractions are still higher than the concentration of neon in the plasma.

In general, there will also be a flux of carbon returning to the divertor surface from the plasma. The gross erosion rate is, therefore, higher than the measured net erosion, and the incident neon flux to give the observed net carbon erosion also would be correspondingly higher. On the other hand, the neon flux onto the surface could be much higher than the neon flux in the SOL due to local recycling of neon at the divertor. A description of net erosion incorporating these important effects requires modeling of impurity transport in the plasma.

In summary, detachment by neon injection, instead of deuterium gas injection, enables reduced divertor heat flux while maintaining reasonable purity of core plasma, lower neutral density at the edge and good H-mode confinement. Neon injection cooled the plasma edge by radiation, reduced the temperature and increased the density of the divertor plasma at the OSP. However, it was found that the net erosion rate of carbon at the OSP was very high (15 nm/s) with neon-detached plasma, in contrast to the absence of erosion from plasmas detached by deuterium injection. A likely cause of the high net carbon erosion rate is physical sputtering by neon, chemically enhanced by the formation of hydrocarbons.

8.6. SMART TILE CONCEPT

A meeting was called to initiate the assessment of Smart Tile, which is a tile that contains multiple diagnostics that could be plugged into different locations in a tokamak chamber. Nineteen diagnostics and corresponding R&D needs were identified that could be used for Smart Tile application. These include the measurements such as plasma current, plasma density, tile current, neutral particle flux, heat flux and the amount of deposited material. A corresponding costing table was also generated for the 19 diagnostics. An initial proposal with budget requests for FY03 and FY04 was completed and sent to the VLT.

8.7. CONFERENCES/MEETINGS

1. Whyte and Wong attended the US-Japan Workshop on high heat flux components and PSI in fusion devices held in Monterey, California. Several papers were presented covering the DiMES program and results, including the lithium and SOL transport experiments that were performed on DIII-D.
2. Whyte participated at the International Tokamak Physics Activities (ITPA) Divertor Meeting that was held at GA. He made one presentation on carbon erosion studies and another one on the erosion from the main chamber wall.
3. Whyte presented an invited talk to 15th PSI conference on “Mitigation of disruption damage using high-pressure noble gas injection”.
4. Wampler of SNL made an oral presented at the 15th PSI conference on the erosion of DIII-D tile from Ne injection.
5. Wong, Whyte, Evans and West attended the 15th PSI conference at Gifu, Japan.
6. Whyte attended the Snowmass meeting and participated in discussions on surface material erosion/redeposition, tritium retention and disruption mitigation.

8.8. PUBLICATIONS

1. W.R. Wampler et al., “Erosion in the DIII-D divertor by neon-detached plasma,” 15th PSI conference, 5/25 to 6/1, Gifu, Japan.

9. RF TECHNOLOGY

9.1. COMBLINE ANTENNA

Charles Moeller arranged for visits with Dr. Seki (NIFS) and Prof. Y. Takase (University of Tokyo) at NIFS on August 22–23, 2002, to participate in comblines antenna discussions and testing. Discussions were held on the measurements NIFS personnel have made on the comblines antenna built for installation on LHD and on a planar prototype version which is easier to model and modify. An individual module of the real comblines antenna and a 10-strap mockup without module-to-module twist are shown in Fig. 9–1. The antenna built for installation on LHD has a twist from one module to the next in order to conform to the vessel wall. Each module consists of a ground plane bar to which a Faraday shield wicket is attached and of a current strap supported at its center by a metal pedestal attached to the center of the ground plane bar. This is the first balanced comblines antenna to be built (previous versions were single ended). In this new comblines antenna, there are two modes possible for each module: an even mode having a current maximum at the pedestal, and an odd mode having a sign reversal of the current at the pedestal. Since these modes are orthogonal, there is not a problem if both sides of the input current strap are driven to excite only the even mode.

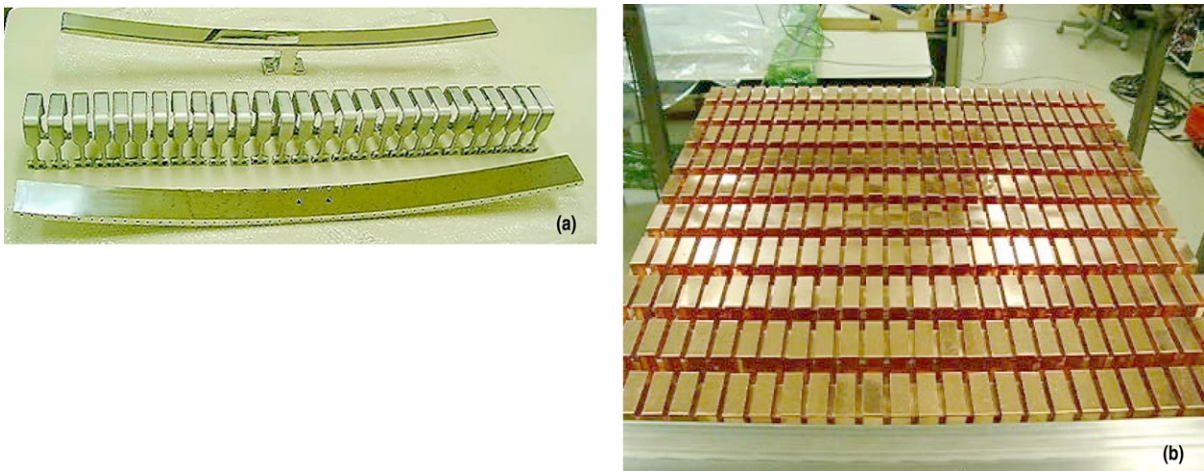


Fig. 9–1. Comblines antenna for use on LHD at NIFS: (a) individual module showing current strap, Faraday shield and back plate, and (b) 10-strap mock-up for testing electrical characteristics.

Low power tests on the real comblines antenna showed that the current distributions were asymmetric and that there were uneven phase shifts from module to module. This indicates

that both modes are propagating, and perhaps also that the ends are not well matched to the feed lines. In tests during the visit, module-to-module spacing on the prototype was increased to account for the twist of the real antenna, and similar behavior was observed. A resonant assembly was made using two of the prototype modules. This allowed for measuring the π and $\pi/2$ resonances for the even and odd modes, which were shown to have the expected current distributions. However, there was some degree of overlap. By adding passive loops, the pass bands could be further separated. It was also demonstrated that exciting both halves of a strap suppresses the odd mode. It was suggested that NIFS consider such balanced excitation for low power testing and, if it works, at high power as well. It does not appear difficult to run a single coax or stripline to the antenna, then split it into two striplines to feed the two halves symmetrically.

9.2. ADVANCED ECH LAUNCHER DEVELOPMENT

As reported previously, GA is developing an advanced mirror under DOE-Advanced Fusion Technology funding. This design uses a copper-plated carbon fiber composite (CFC) mirror with a high thermal conductivity flexible carbon fiber bundle heat pipe emanating from the backside of the mirror. A prototype mirror was fabricated during the third quarter of FY01. In this new mirror, a graded CVD carbon/CFC layer was produced at the mirror surface. A separate flexible carbon fiber bundle with CFC segments at the ends was also produced. During FY02, the CFC disk was coated with a thin layer of titanium and then a layer of copper. The mirror has not yet been tested in a DIII-D ECH miter bend to determine its suitability as an advanced long pulse launcher mirror. The flexible fiber bundle will be used with the CFC mirror or with a small metal mirror to demonstrate its ability to remove heat from the mirror to a heat sink.

JAERI purchased a new 170 GHz prototype remotely steerable launcher apparatus with improved waveguide straightness and dimensional uniformity and with an improved mirror rotation and translation mechanism. The square cross section waveguide has an inner dimension of 45.7 mm, a length of 4.644 m, corrugations on all four walls with a 0.66 mm pitch, and a variation in corrugation depth of less than ± 0.006 mm. The waveguide is made of copper and is vacuum tight so that it can be used at high peak and average power. Low power measurements on the improved waveguide were performed at General Atomics during the third quarter of FY02. The measurements showed that a very large fraction of power (more than 95%) radiated at the intended angle up to 13 deg for either polarization. This compares well for either polarization with the prediction of the basic theory.

Charles Moeller visited JAERI from August 25–30, 2002, to participate in additional low power testing of JAERI's prototype 170 GHz remotely steerable launcher apparatus, with and without miter bends included in the transmission line. Prior to visiting JAERI, Dr. Moeller designed and fabricated an improved apparatus for measuring the far field radiation pattern

from the launcher. The apparatus JAERI had been using allows for computer-controlled scanning in the x-y plane and also performs the data collection. At each desired steering angle, however, the pickup horn had to be manually adjusted to point to the center of the end of the launcher waveguide. The new scanning apparatus positions the pickup horn on the surface of a sphere so that no manual adjustments are necessary, and the horn is always pointed toward the center of the end of the launcher waveguide. The stepper motors brought to Japan turned out to be incompatible with the existing motor drivers. By the time acceptable replacement motors were found, there was no time to finish debugging the system during Dr. Moeller's visit.

Low power measurements made by JAERI personnel using their x-y scanner, however, confirmed excellent steering efficiencies over the range 0 to ± 12 deg for both E and H in the plane of steering, as predicted by theory. With four miter bends inserted in series, with one equivalent straight section removed, however, the losses at ≥ 10 deg were noticeably higher, especially with E in the plane of steering. The reason is related to the effect of the corrugations very close to the miter bend mirror. The corrugations on the walls in the plane of the bend near the mirror cannot be perpendicular to both the incident wave and the reflected wave. This has no apparent effect on the HE₁₁ mode, but may cause conversion of the higher order modes present in the tilted beam. Techniques for minimizing this effect are being evaluated. Results of low power measurements are shown in Fig. 9-2 for the case of no miter bends and E-field in the plane of steering. At the largest steering angle (12 deg) an estimated 97% of the total power is contained in the main beam centered around the 12 deg steering angle.

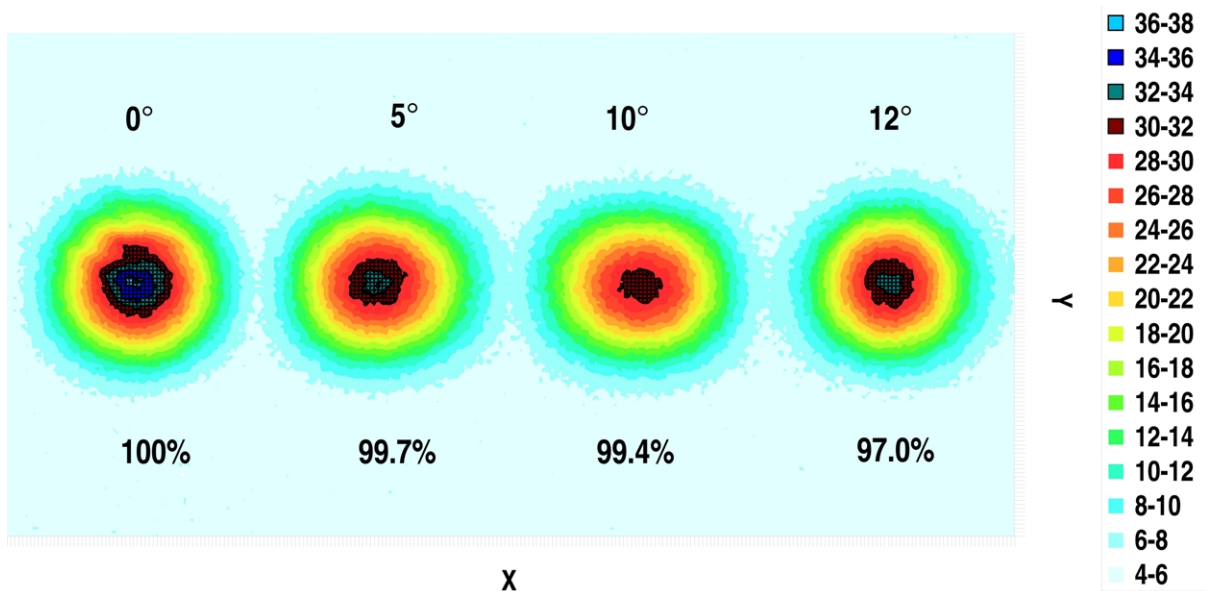


Fig. 9-2. Results of low power measurements made at JAERI on remotely steerable launcher apparatus. For the beam patterns shown, the electric field was in the plane of steering and no miter bends were incorporated in the square cross section length of launcher waveguide.

9.3. INTERNATIONAL COLLABORATION

The 20th U.S./Japan RF Technology Exchange was held from February 28 through March 2, 2002, at the Inuyama International Sightseeing Center near Toki and Nagoya. The host was the National Institute for Fusion Science (NIFS). The meeting was held jointly with the EU-Japan RF Antenna and the Related Technology Workshop. GA staff gave a presentation entitled “Recent Results of the RF Programs at DIII–D and General Atomics.” The U.S. delegation included representatives from DOE Headquarters, ORNL, MIT, and PPPL — these members also gave presentations on their respective programs. Plans were made for U.S./Japan RF Technology collaborations in FY02. Collaborations involving GA include Remote Steering Antenna Testing (with JAERI), Application of Compline Antenna to LHD (with NIFS and University of Tokyo), Reliability of Gyrotron and ECH Transmission Line Components and Windows (with JAERI), and Conducting the U.S./Japan RF Heating Technology Exchange in the first quarter of 2003. The joint meeting with the Europeans provided a forum for discussing the possibility of establishing a formal EU/U.S. RF Technology Exchange. Following the meeting in Japan, the U.S. delegation participated in the U.S.-Korea Fusion Bilateral RF/MW Expert Meeting at KBSI, SAIT and KAERI at Daejeon and at Postech, Pohang, Korea. These discussions explored ways that the U.S. and Korea can collaborate to enhance the rf technology efforts of both countries with emphasis on KSTAR.

The Sixth International ECH Transmission Line Workshop was held at General Atomics’ facilities in San Diego on September 19–20, 2002, in conjunction with the IRMMW 2002 meeting. The workshop was attended by 25 researchers from Germany, Netherlands, Japan, Korea, China and the U.S. GA attendees gave presentations on remotely steerable launcher development, a new fast rotation polarizer miter bend, and performance of the ECH lines at DIII–D.

9.4. CONFERENCES/MEETINGS

1. The 20th U.S./Japan RF Technology Exchange Workshop, Inuyama City, Japan, February 28 through March 2, 2002.
2. The Sixth International Workshop on Electron Cyclotron Resonance Heating Transmission Systems, San Diego, CA, September 19–20, 2002.

9.5. PUBLICATIONS

C.P. Moeller and K. Takahashi, “The Measured Performance of a 170 GHz Remote Steering Launcher,” Proc. 27th Int. Conf. on Infrared and Millimeter Waves, San Diego, California, 2002.

ACKNOWLEDGMENT

This report was prepared for the U.S. Department of Energy under Contract No. DE-AC03-98ER54411.